Complex basin development in a wrench-dominated back-arc area: tectonic evolution of the Crati Basin, Calabria, Italy

V. Spina, E. Tondi, S. Mazzoli

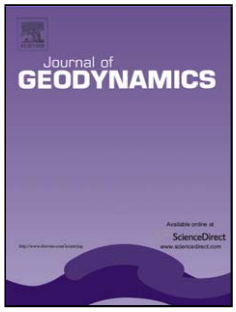

Title: Complex basin development in a wrench-dominated back-arc area: tectonic evolution of the Crati Basin, Calabria, Italy

Authors: V. Spina, E. Tondi, S. Mazzoli

PII: S0264-3707(10)00089-X
DOI: doi:10.1016/j.jog.2010.05.003
Reference: GEOD 1005

To appear in: *Journal of Geodynamics*

Received date: 29-1-2010
Revised date: 11-5-2010
Accepted date: 12-5-2010

Please cite this article as: Spina, V., Tondi, E., Mazzoli, S., Complex basin development in a wrench-dominated back-arc area: tectonic evolution of the Crati Basin, Calabria, Italy, *Journal of Geodynamics* (2008), doi:10.1016/j.jog.2010.05.003

Complex basin development in a wrench-dominated back-arc area: tectonic evolution of the Crati Basin, Calabria, Italy

Spina, V. [1, *]; Tondi, E. [1]; Mazzoli, S [2];

(1) Dipartimento di Scienze della Terra, Università di Camerino, Italy

(2) Dipartimento di Scienze della Terra, Università di Napoli "Federico II", Italy

(*) corresponding author: e.mail: spinavincenzo@yahoo.it fax. +39 06. 61248020

now at:

(1) Total Exploration and Production Italia, via Cornelia 498; 00166, Rome (Italy)

Abstract

Field data and seismic reflection profiles of various resolutions, calibrated by deep well logs, have been used to unravel the tectonic evolution of the Crati Basin (southern Italy). The study area is located in the northern portion of the Calabrian Arc, a well-developed arc-shaped feature of the circum-Mediterranean belts, consisting of a series of ophiolite-bearing tectonic units and overlying basement nappes. NW-SE oriented left-lateral strike-slip faults exerted a major control on the tectonic evolution of northern-central Calabria, from Middle Miocene to Lower Pleistocene times. Such faults, arranged in an *en-échelon* geometry and dissecting the pre-existing Late Oligocene-Early Miocene orogenic belt, led to a structural setting including major N-S striking synforms – as the offshore Paola Basin and the Crati Basin are interpreted based on our results – separated by a broad antiformal ridge. Since the Middle Pleistocene, both E- and W-dipping normal faults developed in the southernmost sector of the Crati Basin, probably as a consequence of both uplift of the orogenic edifice and Tyrrhenian back-arc

extension. The pre-existing regional strike-slip faults became inactive in this sector of the belt. However, working as persistent barriers, it is envisaged here that they inhibited the southern propagation of the newly formed normal faults, which therefore propagated towards the north. A minimum value of cumulative displacement of *ca.* 600 m has been unraveled for the central sector of the Crati Basin since Middle Pleistocene times. This yields a vertical strain rate of *ca.* 0.9 mm/y during the last 700 ka.

Keywords: strike-slip tectonics, extensional tectonics, seismicity, northern Calabria.

1. Introduction

The Tyrrhenian area is considered a classic extensional domain that developed as a result of subduction rollback and related back-arc opening since Late Miocene times (e.g. Malinverno and Ryan, 1986). However, the peculiar modes of development of the Tyrrhenian Sea, controlled by major strike-slip faults accommodating the SE migration of the Calabrian Arc, produced a rather complex tectonic setting (Knott and Turco, 1991). This is characterized by large lateral displacements along NW-SE striking wrench faults (Van Dijk et al., 2000), that are well beyond those typically associated with transfer faults in classic extensional settings. In northern Calabria, in particular, large left-lateral motions along NW-SE lineaments may be associated with geodynamic processes involving the whole subducting slab, with a lithospheric tear starting to develop at ca. 2.5 Ma in this area (Chiarabba et al., 2008).

The Crati Basin (CB), located in the Tyrrhenian side of northern Calabria and traditionally included in the back-arc domain of the Ionian subduction system (Fig. 1), provides a complete stratigraphic and structural record of the various deformation stages that affected the area in Miocene to Quaternary times. The integrated, multidisciplinary analysis carried out in this study allowed us unravelling the polygenic nature of the CB, as well as the relationships between the basin fill and the controlling faults. This sheds new light into the tectonic evolution of back-arc zones strongly influenced by wrench faulting, also allowing to reconcile into a single, coherent picture the apparently contrasting geological information presently available for one of such zones.

The tectonic evolution of the CB and its relationships with the opening of the Tyrrhenian Sea and development of the southern Apennines and the Calabrian Arc are still a matter of debate (Tortorici et al., 1995; Mattei et al., 2002, 2007; Cifelli et al., 2006; Tansi et al., 2007; Pepe *et* al., *in press*). Although various Authors highlighted the importance of extensional tectonics in

northern Calabria no agreement exists on its timing. Trincardi and Zitellini (1987), Mattei et al. (2002 and 2007) proposed that the whole western sector of northern Calabria (i.e. from the Tyrrhenian offshore to the western foothills of the Sila massif) has been undergoing extension since Serravallian time; on the other hand, Bonardi et al. (2005) pointed out that extension must be much younger, since the oldest terrains sealing thrust nappes are Late Tortonian in age.

That extension has been related with opening of the Tyrrhenian Sea, and the CB has been interpreted as a result of back-arc extension (Scandone, 1979). Turco et al. (1990) described the CB as an L-shaped basin as it trends N-S in its southern part (where it is bounded by the morphostructural highs of the Coastal Range and Sila Massif), switching to an E-W orientation in its northernmost part (Fig. 1). The CB is bounded to the south and to the north by long-lived NW-SE trending left-lateral strike-slip faults (Fig. 1). Strike-slip tectonics affected the central-southern Apennines and the Calabrian Arc at different times (Cello and Mazzoli, 1999; Tondi, 2000; Van Dijk et al., 2000; Cello et al., 2003, Tondi and Cello, 2003 and *references therein*). In the southern Apennines, NW-SE strike-slip faults were active since Late Pliocene-Early Pleistocene. However, since the Middle Pleistocene (*ca.* 700 ka), large extensional basins formed along the inner (i.e. SW) side of the southern Apennines as a result of the orogenic collapse (Spina et al., 2008). On the other hand, in the Calabrian Arc NW-SE oriented left-lateral strike-slip faults and associated jog-related features (i.e. folds, reverse/normal faults) controlled the evolution of the belt since Late Miocene times (Knott and Turco, 1991; Van Dijk et al., 2000*, and references therein*).

Recently, Tansi et al., 2007 described transpressive structures formed at compressive jogs related to NW-SE left-lateral strike-slip faults dated as probably Early Pliocene in the southernmost sector of CB. Further evidence of Neogene shortening in the Tyrrhenian sector

of the Calabrian Arc have been recently shown by Pepe et al. (*in press*). These Authors, integrating high-resolution and crustal seismic images constrained by gravity modeling, provided a detailed reconstruction of the architecture of the Paola Basin, which is filled by a thick sequence (ca. 6 km) of Pliocene sediments. Since no significant extensional faults have been observed, the Paola Basin has been interpreted by the Authors as a syncline related to Miocene to Recent continuous shortening. On the contrary, Milia et al. (2009) proposed that the Paola Basin formed during Messinian to Early Pleistocene times as a result of the activity of E-W striking normal faults. According to these Authors, shortening of the basin occurred later, during the Early Pleistocene, and was associated with the activity of left-lateral strike-slip faults. Since the Middle Pleistocene, a change in the slip direction along the NW-oriented faults produced minor pull-apart basins that overprinted the Early Pleistocene folds (Milia et al., 2009).

The previous short review points out how the documentation of different – and in some instances kinematically incompatible – tectonic structures in the western sector of northern Calabria led to different and contrasting tectonic models for the CB, which tried to explain the different roles played by the various structures during the Tyrrhenian spreading related to the Ionian subduction (Tortorici, 1981; Argnani and Trincardi, 1988; Turco et al., 1990; Doglioni et al., 1999; Rossetti et al., 2001; Mattei et al., 2002, 2007; Ferranti et al., 2009; Milia et al., 2009; Pepe et al., *in press*). Recently, the Late Quaternary evolution, both in space and time, of the ~60 km long Crati Fault System has been investigated by Spina et al. (2009). These Authors discussed, in terms of seismic hazard assessment, the interactions among the northern terminations of the Crati Fault System with the NW-trending Pollino fault zone.

In this paper we focus on the architecture of the CB. In particular, we investigate the Miocene to Present space-time evolution of the tectonic structures affecting the basin fill. This is

carried out by integrating geological field data with seismic reflection profiles of various resolutions, calibrated by deep wells. The proposed model contextualizes the evolution of the CB in the regional framework of the western margin of northern Calabria where a series of basins, segmented by the previously mentioned strike-slip structures, occur both offshore (i.e. the Gioia Basin; Sartori, 1989, 1990) and onshore (i.e. the Mesima Graben; Lanzafame and Tortorici, 1981; Tortorici, 1981; Tansi et al., 2005).

2. Regional geological setting

The CB is a tectonic depression located in the western sector of northern Calabria, geologically representing part of the Calabrian Arc (Fig. 1). In the frame of the Mediterranean mobile belt, the Calabrian Arc is an arc-shaped continental fragment located between the E-W trending Sicilian Maghrebides, to the south, and the NW-SE trending Apennines, to the north (Fig. 1a; Ogniben, 1973; Amodio Morelli et al., 1976; Bonardi et al., 2001*and references therein*).

The Calabrian Arc (Fig. 1) consists of a series of thrust nappes composed of tectonic units deriving from the deformation of different palaeogeographic domains. The backbone of the Calabrian Arc is composed of Palaeozoic crystalline rocks, which have been interpreted either as basement units belonging to the African continental margin (Grandjacquet and Mascle, 1978 *and references therein*), or as part of the European palaeo-margin (Bouillin et al., 1986 Dewey et al., 1989). Since the Oligocene, these basement rocks thrusted onto ophiolite-bearing units of the Neotethys domain. Since the Early Miocene, the whole tectonic edifice over-thrusted carbonate platform rocks of the Apulian continental margin (Dewey et al., 1989; Bonardi et al., 2001; Rossetti et al., 2001; Mattei et al., 2002; Bonardi et al., 2005; Iannace et al., 2005).

The evolution of the Calabrian Arc is characterized by its progressive southeastward migration associated with Africa-Europe major plate convergence (e.g. Mazzoli and Helman, 1994), oroclinal development of the Apennine-Calabrian-Sicilian belt (e.g. Johnston and Mazzoli, 2009) and/or roll-back of the Ionian slab (Goes et al., 2004; Guarnieri, 2006). These processes led to the progressive opening of the Tyrrhenian basin in the area of back-arc extension (Tortorici, 1982; Malinverno and Ryan, 1986; Knott and Turco, 1991; Catalano et al., 1993; Doglioni et al., 1999; Van Dijk et al., 2000; Guarnieri, 2006; Johnston and Mazzoli, 2009).

The progressive migration of the Calabrian Arc towards the southeast occurred, since Middle Miocene times, along a NW-SE to WNW-ESE-trending regional strike-slip fault system characterized by left- and right-lateral movements in the northern and in the southern sector of the Calabrian Arc, respectively (Fig. 1; Ghisetti and Vezzani, 1982; Turco et al., 1990; Knott and Turco, 1991; Catalano et al., 1993). Such faults, dissecting the pre-existing thrust sheets, played an important role in the Neogene-Quaternary geodynamic evolution of the Central Mediterranean area. Based on structural studies supported by seismic and bore-hole data, Van Dijk et al. (2000) proposed that the whole tectonic system consisted of Middle Miocene-Early Pleistocene crustal transpressional fault zones, mainly dipping towards the NE, characterized by left-lateral and reverse kinematics (Fig. 1 b). Along these structures, in correspondence of their restraining bends, extrusion of the deep-seated units of the Calabrian Arc together with underlying Mesozoic carbonate rocks have been recently described by Tansi et al. (2007).

Since the Middle Pleistocene, a strong regional, still active uplift affected the northern Calabrian Arc. This has been interpreted as the isostatic response to the removal of the high-density mantle/lithosphere root, due to detachment of the Ionian subducted slab (Westaway,

1993; Wortel and Spackman, 1993; Tortorici et al., 1995). According to these Authors, the regional uplift was coupled with the formation of a series of grabens along the entire western sector of the Calabrian Arc. The geometry of this rift zone (the so-called Siculo-Calabrian Rift Zone, *sensu* Monaco and Tortorici, 2000) would be outlined by the distribution of the epicentres of the largest historical (X-XI MCS, 6<M<7.4) crustal earthquakes in the region (CPTI, 2004; DISS, 2009). The CB, forming part of this zone, is bounded by the Coastal Range to the west, by the Sila Massif to the east, and by the Pollino Ridge to the north (Fig. 1). The basin is morphologically asymmetric with a steeper and shorter fluvial drainage along its eastern border, and the Crati River flowing along the easternmost side of the valley. Based on structural and anisotropy of magnetic susceptibility (AMS) studies, Rossetti et al. (2001) and Mattei et al. (2002) outlined an extensional regime in the central portion of the Calabrian Arc since Late Miocene times. Such a tectonic regime, characterized by a consistent WSW-ESE stretching direction, would have originated normal faults striking on average NNE-SSW. According to these Authors, no shortening would have occurred in the CB since Late Miocene times. Other workers (i.e. Vezzani, 1968; Lanzafame and Zuffa, 1976; Tansi et al., 2007) recognized compressional structures in various sectors of the CB, which they have interpreted either as a result of distinct compressional tectonic phases, or formed in correspondence of jogs related to NW-SE left-lateral strike-slip faults. On the other hand, Turco et al. (1990) interpreted the CB should as a fault-bounded basin including a series of distinct depocentres comprised between NW-SE striking left-lateral faults. More recently Tansi et al., (2007), based on the mathematical elastic-plane model of Xiaohan (1983), proposed that the formation of the normal fault-related CB could be kinematically compatible with the *en échelon* right-stepping configuration of the previously mentioned NW-SE left-lateral strike-slip faults, being controlled by stress re-distribution and re-orientation.

3. Field data

Regional mapping of the CB has been integrated with detailed lithostratigraphic logging, biostratigraphic and meso-scale structural analyses in order to constrain age, geometry and kinematics of the tectonic features affecting the basin infill and to investigate the whole structural setting of the area.

3.1 Basin stratigraphy

The CB is filled by Upper Miocene to Holocene clastic marine and fluvial deposits (Fig.2, see also Vezzani, 1968, Colella et al., 1987) covering the Palaeozoic crystalline bedrock, in the southern part of the basin, and Meso-Cenozoic carbonates in its northern sector (i.e. in the Pollino area). The original stratigraphic contact between the basin infill and its bedrock is still well exposed all along the western side of the Sila Massif (Lanzafame and Zuffa, 1976). Although the main depocentre is located in the northernmost sector of the basin (Sibari Plain, see Fig. 1), the thickness of the deposits increases from the Coastal Range towards the Sila foothills (Fig. 2 c). Published stratigraphic data are mainly from specific sectors of the basin; however it has been proposed that the whole basin fill consists of two main depositional sequences bounded by a regional angular unconformity. The first sequence, Late Miocene to Early Pliocene in age, is characterized in the structural highs by a Messinian unconformity, whereas the second one, spanning from the Middle-Late Pliocene to the Pleistocene, is represented by distinct lithofacies grading one into another both vertically and laterally (Di Nocera et al.; 1974; Romeo and Tortorici, 1980).

In this study, basin infill has been sub-divided in four major synthems (Fig. 2 a). Each synthem is bounded by an angular unconformity, corresponding to an erosional surface

and/or to a depositional hiatus, probably related to tectonic activity. Different stratigraphic units have been identified based on both age of the deposits and litostratigraphic characteristics. The age of the deposits has been determined by means of new biostratigraphic analyses integrated with published data.

3.1.1 Basal Synthem (BaS)

This synthem is characterized by Upper Miocene deposits cropping out mainly in the southernmost part of the basin and, sparsely, along the foothills of the Coastal Range (Fig. 3 b). Small outcrops of sediments belonging to the BaS have been also described along the Sila foothills by Lanzafame and Zuffa (1976).

The BaS consists of conglomerates gradually evolving upwards to sands and arenites. The latter sediments, in turn, give way upwards to clays and silty clays, and then to Messinian evaporites (Lanzafame and Tortorici, 1981). The thickness of the BaS is variable: Lanzafame and Tortorici (1981) suggested 250 m; however, the whole thickness increases to the north as confirmed by subsurface data.

3.1.2. Pliocene Synthem (PS)

The PS consists of two thinning-upward sub-synthems bounded by discontinuities and depositional hiatuses (Fig. 2), cropping out mainly along the western border and the northernmost part of the CB (Fig. 3).

The first sub-synthem (1Ps) unconformably overlies sediments belonging to the BaS as well as pre-Neogene rocks belonging to the thrust sheets forming the basin substratum (Fig. 3, see also Lanzafame and Zuffa, 1976).

The related deposits consist of cross-bedded continental conglomerates, progressively evolving upwards to sands with planar bedding. Marine clays characterize the top of the interval. Biostratigraphic analyses (Table 1) suggest a Zanclean age (biozone MPL3; *Globorotalia margaritae-puncticulata sensu* Rio *et al.,* 1991; Sprovieri, 1992) for these sediments, in agreement with that proposed by Spina et al. (2009). The facies are probably braided river deposits, where fluvial conglomerates are interfingering with silts, sands and marine clays. The observed thickness varies between zero to the south, to about 200 m in the north (Lanzafame and Tortorici, 1981).

Sediments of the second sub-synthem (2Ps) overlie both the Miocene and the Lower Pliocene deposits (Fig. 3). To the south, 2Ps is characterized by fluvial and fan-delta conglomerates evolving, towards the axial part of the basin, to marine silty clays. Based on geological considerations, Spina et al. (2009) proposed a Middle-Upper Pliocene age for these clays. Biostratigraphic analyses (Table 1) point out a Piacenzian age (biozone MPL5a; *Globigerinoides elongatus sensu* Rio et al., 1991; Sprovieri, 1992). This age is at variance with that proposed by Vezzani (1968), who suggested a Lower Pleistocene age for these deposits.

In the northernmost part of the basin (Fig. 3 a), marine silty clays overly Messinian deposits or Mesozoic carbonates. Based on surface data, the 2 Ps can be estimated as *ca.* 400 m thick (see also Russo and Schiattarella, 1992).

Wells for hydrocarbon exploration (see section 4), located in the northernmost part of the basin, showed that the whole PS unconformably overlies Messinian deposits and is characterized by a strongly variable thickness, probably related with the existence of structural highs and depressions.

3.1.3. Plio-Pleistocene Synthem (PPS)

PPS crops out extensively along both margins of the basin (Figs. 2 c and 3); in particular the deposits of this synthem unconformably cover older sediments along the western border of the CB (Figs. 2 c and 3 b), resting directly also on Palaeozoic crystalline rocks along the eastern margin of the basin (Figs. 2 c and 3 b; see also Carobene and Damiani, 1985). To the north, these sediments cover Mesozoic carbonates (Fig. 3 a). In the southernmost sector of the CB, the bottom of PPS is mainly characterized by fossiliferous calcarenites with planar cross bedding; however, along the Sila foothills, this succession starts with conglomerates evolving upwards to thin sands (Fig. 2 c). All such deposits grade into marine silty clays, cropping out in the axial and main depocentral sector of the basin (Fig. 2). Clays sampled in the Section 3 (see Table 1), have been tentatively assigned to the Gelasian, (biozone MPL6, *Globorotalia inflata, sensu* Rio et al., 1991; Sprovieri, 1992) by means of biostratigraphic analyses.

However, geological considerations and the generalized occurrence of *Hyalinea baltica* unraveled also by new analyses allow assigning an Emilian age (biozone *Globigerinoides quadrilobatus*) to these clays. In the northernmost part of the CB, coarse-grained sediments overlying the Pleistocene clays crop out in the peripheral areas of the basin (Fig. 3 a) and along the Ionian coast of Calabria (Vezzani, 1968). The thickness of the PPS increases towards the Sibari Plain, as shown also by deep wells for hydrocarbons exploration (see section 4).

3.1.4. Pleistocene Synthem (PlS)

These deposits crop out along the axial part of the basin and, more extensively, in the Sibari Plain (Fig. 3). This synthem consists of Gilbert-type marine fan delta deposits (Colella,

1988, and *references therein*), which represent the sedimentary response to a strong differential uplift involving the basin margins and the basin itself. In particular, Colella et al. (1987) proposed that different fan delta bodies prograded into small fault-controlled sub-basins within restricted gulfs and narrow embayments of the CB.

PIS deposits show an erosional contact with older deposits in the peripheral sectors of the southern part of the CB (Fig. 2 b, c), but they rest conformably onto the Lower Pleistocene clays in the axial part of the basin. Based on the stratigraphic relationships with underlying deposits, we suggest an Early-Middle Pleistocene age for the fan delta conglomerates. This is in good agreement with the age proposed by previous workers (Russo and Schiattarella, 1992). The observed thickness for this interval, in the southernmost part of the basin, is about 150 m and increases towards the north. Middle Pleistocene cryoclastic breccias (Fig. 3 a, see also Perri and Schiattarella, 1997) also occur along the foothills of the Pollino Range. In the Sibari Plain (Fig. 3 a) the fan delta conglomerates pass upwards to Upper Pleistocene lacustrine/palustrine sediments (see also Busquet and Gueremy, 1969), clearly pointing out the regressive trend of this interval. Lacustrine sediments attain a maximum thickness of about 100 m.

3.2. Structures

Both compressional and extensional tectonic features deform sediments of different age within different sectors of the CB. In the southern and central part of the basin, roughly N-S trending asymmetric anticlines involve sediments of Miocene and Lower Pliocene age (up to the 1Ps, Fig. 4 a). At the outcrop scale, related reverse faults and minor folds display dominant NNW trends (Fig. 4 a). In the northern sector of the basin, minor high-angle reverse faults affect Lower Pleistocene fan delta conglomerates (Fig. 4 b), as also described by other

authors (Busquet and Gueremy, 1969; Lanzafame and Tortorici, 1981; Monaco *et al.,* 1996; Schiattarella, 1996, 1998). In the same area, along the Pollino Fault Zone, Mesozoic carbonates are locally brought into contact with Lower Pleistocene conglomerates by means of high-angle reverse faults (Fig. 4 c). Minor NW-striking, left-lateral strike-slip faults have been observed within breccias of probably Early Pleistocene age (Fig. 4 d). Notwithstanding the occurrence of such minor structures in the northern part of the basin, the morphology of the CB is clearly controlled by a N-S trending structural grain along both sides of the basin abutting against long-lived strike-slip fault zones (Fig. 5 a, b). The western border of the basin is characterized by three main N-S striking, E-dipping normal faults (Figs. 3 b, 5 a) arranged in an *en-échelon* geometry: the 15 km long Montalto Uffugo-Rende Fault (MRF); the 25 km long San Marco Argentano-San Fili Fault (MMF), and the 8 km long Fagnano Fault (FF). These left-stepping and overlapping faults are characterized by impressive morphological scarps (Fig. 5 a) and severely tilted strata have been observed within the fault relay ramps. In the central and southern sectors, the eastern border of the basin is characterized by a series of N-S oriented structural lineaments strongly controlling the drainage pattern (Fig. 3 b). Instrumental seismicity and medium-intensity historical earthquakes cluster along these lineaments, which have been already interpreted as active faults (Tansi et al., 2005; Spina et al., 2009 *and references therein*).

Our field survey confirmed that the N-S structural grain corresponds with tectonic structures affecting the crystalline bedrock and, in some case, also sediments of the basin infill (Fig. 6, see also Carobene and Damiani, 1985). This confirms that also this margin of the basin is affected by fault strands characterized by minor (i.e. < 50 m) throw, locally slightly displacing the original onlap contact between basin sediments and basement crystalline rocks (Fig. 3 b).

An accurate estimate of displacement associated with the basin-bounding normal faults based on the geological offset is rendered difficult by the fact that these faults mainly put into contact crystalline rocks against clastic sediments (Fig. 3 b), therefore hindering the correlation of footwall and hanging-wall cut-offs across the structures. However, some Authors (Piccardi et al., 1999; Cello et al., 2003; Ganas et al., 2004, Spina et al, 2008; Spina et al. 2009; Petit et al. *in press*) observed that the height of the first order triangular facets roughly approaches the long-term activity of basin-bounding normal faults. The morphological offset of the faults bordering the western side of the basin (i.e. the height of the steepest part of faceted spurs, see Fig. 5 a) ranges between 60 m and 230 m (see also Tortorici et al., 1995, Spina et al., 2009), with the highest values clustering in the central part of the array and the minimum values occurring at relay ramps. Along the eastern border of the basin the morphological offsets observed along faults range between 50 m and 170 m, decreasing rapidly to 0 towards the Pollino Range (Fig. 5 f). Extensional structures, oriented mainly N-S, also affect the interior part of the basin and cross-cut, at the meso-scale, compressional structures deforming the basin infill. In the southern sector of the CB, normal faults affecting Lower-Middle Pleistocene conglomerates show evidence for syn-sedimentary activity (Fig. 5 c, d and e), especially in the axial zone of the basin.

A structural survey has been carried out in order to investigate in detail the kinematics of the extensional faults. Fault data have been collected both along the sparse, morphologically fresh, fault plane outcrops of the basin bordering structures and in the basin interior. In the southern and central sectors of the basin the detected structures include faults showing dip angles in the range of 50°-70° (Figs. 6 and 7), mainly striking NNW-SSE and NNE-SSW, with a statistical peak strike value of N11°E (Fig. 7). Further faults are NE-SW trending, with a statistical peak strike value of N55°E (Fig. 7). All together, the collected faults show oblique-

slip to pure dip-slip kinematics, with pitch values ranging between 55° and 90° (Fig. 7). No consistent superimposition of striae/shear fibres has been observed on fault planes, thus suggesting that no major switch of the regional stress field occurred in this area after the formation of these structures. The direction of extension in this part of the CB, as shown by fault slip inversion for palaeostress analysis (Reches, 1987), is sub-horizontal and oriented E-W (Fig. 7), with an average angular divergence of 22° (Fig. 7). The low value of the axial ratio (R=0.22), suggests a geometry of the stress field characterized by similar values of σ2 and σ3.

In the northern part of the CB normal faults cross-cut compressional structures and affect sediments of Middle-Late Pleistocene age. In this area extensional faults strike NNW-SSE, with a mean peak strike value of N348°E (Fig. 7), and exhibit an elliptical profile of displacement (Fig. 5 f, g) as they loose their morphological evidence approaching the Pollino Fault Zone (Fig. 5 f). These normal faults are characterized by oblique-slip kinematics showing a left-lateral component of motion (see Fig. 5 g and Fig. 7 b). Both pitch of the *striae* and asymmetric profile of displacement are characteristic of the tip zones of basin-bounding normal faults, as suggested by several Authors (Roberts and Ganas, 1996; Scholz and Gupta, 2000; Roberts et al., 2004). Inversion of fault slip data point out a sub-horizontal, NNE-SSW oriented maximum extension direction in the northernmost part of the CB (Fig. 7 b), with an average angular divergence of about 6° (Fig. 7 b). The low value of the axial ratio (R=0.12) indicates a geometry of the stress ellipsoid similar to that characterizing the southern part of the basin.

4. Subsurface data

Sparse subsurface data from the oil industry are available for the CB. Well logs, mainly concentrated in a relatively small area within the Sibari Plain, were used to assess the thickness of sedimentary formations in this sector. Four 2D seismic lines, that were shot about twenty years ago for HC exploration, are also available. Due to the relatively poor quality of the lines, their wide spacing and limited area coverage, this dataset does not allow fully constraining the structures in 3D (i.e. defining precisely fault strike and length) throughout the entire basin. Nevertheless, these data are useful to describe the overall subsurface geometry of the CB and the structures controlling the basin architecture.

4.1. Well data

Well data show clearly how the Sibari Plain has been an area of sediment accumulation since Miocene times. The pre-Miocene bedrock has been reached by one of the wells (Crati 3 well, Fig. 8), probably due to the occurrence of a local structural high interposed between tectonic depressions characterized by major accumulation of sediments. Based on the well logs, the thickness of the Miocene sediments in the northernmost part of the basin is likely to be largely in excess of 500 m. Messinian evaporites (the so-called *Gessoso-Solfifera Fm*; Di Nocera et al., 1974 and *references therein*) have been found at similar depth in all the wells with the exception of the Crati 3 well, which did not encounter such sediments (Fig. 8). This suggests that evaporites formed isolated ponds, probably confined within structural depressions. Pliocene clays and marls, encountered in two wells (Crati 1 and Crati 2), are characterized by a thickness ranging between *ca.* 90 m and 400 m (Fig. 8). Pleistocene sediments unconformably cover almost the whole CB, with a thickness of about 1000 m (Fig. 8), sealing a complex palaeo-morphology.

Sonic logs, available for the Ogliastrello and Thurio-1 wells, have been used to constrain velocity intervals within the sediments (Fig. 9). The quality of the data is not very high; however, velocity data estimated for similar sediments in the Tyrrhenian offshore by Milia et al. (2009) can be used for comparison. Velocity within Pleistocene clays and sandy clays, in general obviously increasing towards the bottom of the formation, ranges between 1800 m/s to 2300 m/s (Fig. 9). An average value of 2000 m/s has been considered to be representative for these sediments. This is in good agreement with the value used for Plio-Quaternary sediments in the Paola Basin by Milia et al. (2009). A value of 2000 m/s has been taken to be representative also for Late Pliocene sediments encountered in the Crati-1 and Crati-2 wells (Fig. 8). Velocity in Miocene sediments (characterized by sands and conglomerates covering evaporitic sediments in the Ogliastrello and Thurio-1 wells) ranges between 2300 m/s and 3300 m/s (Fig. 9). An average value of 2700 m/s, slightly lower than that proposed by Milia et al. (2009), has been considered for these deposits.

4.2. Seismic lines

Three NE-SW oriented seismic reflection profiles are available across the Sibari Plain. They have been calibrated using the wells that were drilled in order to test Miocene structural traps and shallower Plio-Quaternary targets (Fig. 10). A further seismic line, roughly oriented E-W and almost orthogonal to the major structures bordering the CB, allowed us investigating also subsurface structure of the central portion of the basin (Fig. 10). However, while seismic lines could be tied to well logs in the northernmost part of the basin to constrain geological horizons, no exploration wells are present in the central sector of the basin and no offset exists between seismic lines in this area and those to the north. Therefore, we used surface information (i.e. the geological map) and the characteristics of the seismic facies to

differentiate between major stratigraphic units in the central basin area. Despite this approximation, basin architecture, type and overall kinematics of the structures deforming the basin fill could still be recognized with confidence.

In the northern sector of the basin, a high-amplitude event (calibrated by well logs) marks the top of the Miocene sands. The top of the Messinian evaporitic sediments can also be recognized in the line CS 304-81. The whole Miocene succession slightly thickens to the northeast, probably as a result of fault activity (Fig. 10). No Pliocene deposits have been encountered in the well Thurio-1 (see Fig. 8). This suggests that the seismic line CS-304-81 is almost coincident with a morphological or structural threshold separating Pliocene depocentres located to the southwest (see Pliocene horizons recognized in seismic lines CS-306-81 and CS-323-83) and possibly to the north, all of them being unconformably overlain by Pleistocene sediments. Evidence of compressional tectonics can be recognized in the seismic lines from the northernmost part of the basin (Fig. 10), where roughly WNW-ESE striking reverse faults, probably reactivating pre-existing normal faults, have been interpreted. Some minor reverse faults detach at the level of the Messinian evaporites (Fig. 10). Reverse faulting also produced deformation of the Lower Pleistocene reflectors (which, in some instances, are offset), suggesting Early Pleistocene age reverse fault activity (Fig. 10).

The seismic line CS-103-90H-FR crosses the central sector of the basin, from the Coastal Range to the Sila foothills. The metamorphic basement, characterized by a high-amplitude discontinuous reflector, effectively defines the shape of the CB. Miocene sediments, characterized by high-amplitude reflectors displaying moderate lateral continuity, occur throughout the whole seismic line. The Top-Miocene reflector is very shallow along the western border of the basin (i.e. Coastal Range foothill), deepening to 1.8 s TWT in the central sector of the seismic line and eventually shallowing again towards the eastern side of

the basin. These deposits reach the maximum thickness (*ca.* 0.25 s TWT) in the central sector of the line; taking into account the average velocity estimated for this interval (see Fig. 9), the Miocene sediments result about 330 m thick in the main basin depocentre area. Pliocene sediments, characterized by medium- to high-frequency reflectors showing moderate lateral continuity, overlap the Miocene sediments. Due to the lack of wells allowing tying with the seismic line, the interpretation of the top of the Pliocene has to be considered as tentative. Therefore, although a general deepening of these sediments can be observed in the seismic line, no definitive information about the thickness of this interval can be obtained. Pleistocene deposits are characterized by high-frequency, high-amplitude reflectors displaying good lateral continuity. Onlap relationships with the underlying strata have been tentatively used to identify the bottom of these deposits. Pleistocene sediments thicken towards the east, depicting a growth-geometry against a series of west-dipping normal faults. Based on such assumptions, a *ca.* 1.3 s TWT thick package of Pleistocene sediments can be interpreted in the seismic line. Taking into account the average velocity of this interval (Fig. 9), a thickness of about 1200 m may be estimated for the Pleistocene sediments. The whole Miocene to Quaternary basin fill thickens towards the basin depocentre, reaching a thickness of *ca.* 1.9 sec TWT (i.e. *ca.* 2200 m).

A series of extensional faults controlled the accumulation of Pleistocene sediments, as demonstrated by the fan geometry observed in the seismic profiles. Although the 3D geometry of the structures cannot be fully constrained, it may be envisaged that these faults are roughly N-S trending, parallel to the main structures bounding the basin at surface.

Seismic line CS-103-90HFR (Fig. 10) shows that, in its central sector, the basin fill is controlled by a W-dipping master fault and associate fault splays located along the axial zone of the Crati River valley. The reflectors interpreted as the possible base of the Pleistocene

deposits are cumulatively displaced vertically by about 0.5 s TWT, corresponding to a value of about 600 m of vertical offset.

5. Discussion

The CB is part of a series of basins located along the Tyrrhenian side of the Calabrian Arc. According to Monaco and Tortorici (2000), these basins (including the Mesima and Gioia basins; Fig. 11) are part of the Siculo-Calabrian Rift Zone, a sector undergoing crustal extension where basin-bounding normal faults produced strong ($M \geq 6.5$) historical earthquakes and still release seismic energy (Fig. 11 a, b). The extensional basins are segmented by long-lived, NW-SE striking left-lateral fault zones. The various basin segments exhibit different trends (Fig. 11). Although the recent tectonic evolution of these basins is generally accepted by most of the Authors, as it was mentioned previously their structural style and tectonic setting are still strongly debated (compare, for instance, Tortorici et al., 1995; Mattei et al., 2002; Cifelli et al., 2006; Mattei et al., 2007; Tansi et al., 2007; Milia et al., 2009; Pepe et al., *in press*). The documentation of different, and in some instances kinematically incompatible tectonic structures in the western sector of northern Calabria led to different and contrasting tectonic models, which tried to explain the different role played by the structures during the Tyrrhenian spreading related with the Ionian subduction system. The contractional structures affecting Middle Miocene to Lower Pleistocene deposits in different sectors of the CB have been generally interpreted as evidence of distinct compressional tectonic phases that would have occurred within a framework of generalized extension (Vezzani, 1968; Lanzafame and Zuffa, 1976; Lanzafame and Tortorici, 1981; Ghisetti and Vezzani, 1982; Knott and Turco, 1991). More recently, Tansi et al. (2007) described compressional structures formed in correspondence of compressional jogs of NW-SE left-

lateral strike-slip faults along the western sector of northern Calabria. Following the mathematical elastic-plane model proposed by Xiaohan (1983), these Authors proposed that the CB could be interpreted as a fault-bounded extensional basin. This, being kinematically compatible with NW-SE left-lateral strike-slip faults, according to the Authors, would have formed as a consequence of stress re-distribution along transcurrent fault zones. On the other hand, the kinematic compatibility of a N-S oriented extensional basin (i.e. the CB) with NW-SE tending left-lateral strike-slip faults is clearly problematic, as the latter would be associated with roughly E-W trending compression, rather than extension.

Based on the data exposed in this paper, we propose an alternative tectonic interpretation for the CB within the framework of the regional geological picture of northern Calabria (Fig. 12). In the study area, the oldest marine sediments are Tortonian in age and crop out along both the Tyrrhenian margin of northern Calabria and the Ionian coast, directly overlying crystalline units. Petrographic data suggest that the source for these sediments was a morphological high coincident with the present-day Sila Massif (Critelli, 1999). At that time, the Sila Massif would have represented part of a wide emerged area supplying clastics to basin areas located both to the west and to the east of the range. This hypothesis is confirmed by apatite fission track data, indicating exhumation of the Sila block between 35 and 15 Ma (Thomson, 1994). The Messinian sediments, mainly characterized by evaporitic facies, extensively cover the Tortonian deposits in the Tyrrhenian offshore. Within the CB Messinian sediments crop out mainly along a narrow belt at the foothills of the Coastal Range and have been found in some wells in the Sibari Plain (Fig. 8). This suggests that one or more morpho-structural highs, in part coincident with the present-day Coastal Range, separated the Tyrrhenian basin from a smaller eastern basin during the Late Miocene. These structural highs (proto-Coastal Range in Fig. 12) represented wide growing anticlines forming along transpressive structures,

kinematically linked with NW-SE strike-slip fault zones (like FCFZ and AGFZ in Fig. 12 and in Figs. 5 b, see also Tansi et al., 2007). These anticlines controlled the configuration and the evolution of both the Paola Basin (Pepe et al, *in press*) and also the CB (Fig. 12 e). The latter basin, in particular, developed as a large growing syncline, as demonstrated by the overall geometry of the Miocene-Pliocene sediments in the central sector of the basin (seismic line CS-103-90H-FR; Fig. 10). This tectonic setting is also suggested by the basin architecture and by the geometry and kinematics of the structures observed in the field, deforming the basin fill (i.e. thrust faults and N-S trending folds).

The Lower Pliocene deposits are of marine type, as suggested by both facies and microfossiliferous data. This could indicate that the proposed morpho-structural high (i.e. the Coastal Range), already partially developed and still growing during the Early Pliocene, divided the Tyrrhenian basin from the proto CB (Fig. 12 a, b), which was connected northwards with an open basin (i.e. the Ionian Sea). Evidence of possible Early Pliocene push-ups along strike-slip fault zones (i.e. FCFZ and AGFZ in Fig. 12) has been provided by Tansi et al. (2007). This suggests an ongoing activity of NW-SE tending fault zones and associated structures in this sector of the Calabrian Arc.

During the Early Pleistocene the CB was still fed from north. Deposition occurred in a transitional environment (i.e. Gilbert-type fan delta) along the axial part of the basin, hence suggesting a general regressive trend. Early Pleistocene compressional structures in the Sibari Plain are unraveled by seismic interpretation (Fig. 10). These structures probably re-activated older (i.e. Miocene) normal faults. In the field, compressional structures have been observed affecting Lower Pleistocene deposits within the northernmost part of the CB (Fig. 4 b) and along the Pollino Fault (Fig. 4 b, c).

Since the Middle Pleistocene (i.e. 700 Ka) a generalized regional uplift affected the entire western sector of the Calabrian Arc (Russo and Schiattarella, 1992; Schiattarella, 1998). This is associated with an extensional tectonic regime recognized throughout the whole southern Apennines (Ortolani *et al*., 1992; Schiattarella, 1996, 1998 *and references therein*). According to Tortorici et al. (1995) the normal faults bounding the western margin of the CB are characterized by a slip rate of *ca.* 1 mm/a since the Middle Pleistocene and are responsible for the Coastal Range uplift. From the Middle Pleistocene onwards normal faults started to affect the CB and also the eastern border of the Paola Basin (Pepe et al., *in press*., Fig. 12 c, d). Nonetheless, a more complex tectonic regime is thought to be active at the Present-day farther to the west in the Tyrrhenian offshore (Pepe et al., *in press*. Fig. 12 e).

Based on the different age of the structures observed within various sectors of the CB, we propose that normal faults bounding the basin propagated mainly towards the north (Fig. 13; Spina et al., 2009) as a consequence of the presence of long-lived NW-SE striking strike-slip faults which inhibited their southwards propagation (Fig. 13). In particular, Pizzi and Galadini (2009) demonstrated that pre-existing crustal structures are able to hinder fault re-activation and propagation, therefore controlling the maximum length of Quaternary normal faults in the central and northern Apennines. In the same way we propose that long-lived fault zones in the northern Calabrian Arc could behave as persistent segment boundaries (*sensu* Pizzi and Galadini, 2009) and could have partitioned, at a regional scale, the whole regional back-arc extension among a series of extensional basins (Fig. 11).

Keeping into account the cumulative displacement of the reflectors ascribed to Pleistocene sediments in the central sector of the CB, a vertical strain rate of about 0.9 mm/a may be estimated for the extensional faults controlling the basin architecture since the Middle Pleistocene (i.e. since 700 Ky). The latter value, which is in good agreement with that

obtained by Tortorici et al. (1995), has to be considered as a minimum value, because it is not possible to estimate the displacement accumulated along basin bordering normal faults since the Middle Pleistocene.

6. Conclusions.

In this paper we focused on the architecture of the Crati Basin by integrating geological field data and seismic reflection profiles of diverse resolutions, calibrated by means of deep well logs. The integrated data sets allowed us investigating the space-time evolution of the tectonic structures affecting the basin fill from Miocene to Present.

The study area is located in the northern portion of the Calabrian Arc, whose evolution was controlled by regional NW-SE trending left-lateral strike-slip faults from Middle Miocene to Middle Pleistocene times. These faults, arranged *en-échelon* and dissecting the preexisting (Late Oligocene-Early Miocene) orogenic belt, controlled the development of N-S striking, broad antiformal ridges (i.e. the Coastal Range) and associated regional synforms such as those forming the Paola Basin, in the Tyrrhenian offshore, and the Crati Basin onshore. Since the Middle Pleistocene, both E- and W-dipping normal faults formed in the southernmost sector of the Crati Basin. The inherited regional strike-slip faults became inactive in this sector of the belt and behaved as persistent barriers, inhibiting the southern propagation of the newly formed normal faults. As a consequence, the N-S striking normal faults propagated northward. The cumulative fault displacement in the central sector of the Crati Basin is about 600 m since the Middle Pleistocene, yielding a minimum vertical slip rate of *ca.* 0.9 mm/y.

The integrated, multidisciplinary approach used in this study allowed us obtaining a comprehensive picture of the various stages of development of the Crati Basin, as well as the related structural controls. Our results provide new insights into the tectonic evolution of back-

arc zones strongly influenced by wrench faulting, a geodynamic setting that may be envisaged as characterizing areas of extreme arc development and migration, similar to the Calabrian Arc.

Acknowledgments

Biostratigraphic analyses have been partially carried out by Stigliano D. and Tripodi A. as part of their MSc thesis. 3D views used in the figures are from Google Earth™ (vertical exaggeration 3x). Thorough and constructive reviews by two anonymous referees helped to improve the manuscript.

References

Amodio Morelli, L., Bonardi, G., Colonna, V., Dietrich, D., Giunta, G., Ippolito, F., Liguori, V., Lorenzoni, S., Paglionico, A., Perrone, V., Piccarreta, G., Russo, M., Scandone, P., Zanettin Lorenzoni, E., Zuppetta, A.., 1976. L'arco Calabro-Peloritano nell'orogene appenninico Maghrebide. Memorie della Società Geologica Italiana, 17, 1-60.

Argnani, A., Trincardi, F., 1988. Paola slope basin: evidence of regional contraction on the eastern tyrrhenian margin. Memorie della Società Geologica Italiana, 44, 93-105.

Bonardi, G., Cavazza, W., Perrone, V., Rossi, R. 2005. Calabria-Peloritani Terrane and Northern Ionian Sea. In: G.B. Vai, I.P. Martini (eds.) Anatomy of an Orogen: The Apennines and Adjacent Mediterranean Basins, 287-306. Kluwer Academic Publishers, Dordrecht/Boston/London.

Bonardi, G., De Capoa, P., Di Staso, A., Perrone, V., Sonnino, M., Tramontana, M. 2005. The age of the Paludi Formation: a major constraint to the beginning of the Abulia verging

orogenic transport of the Northern sector of the Calabria-Peloritani Arc. Terra Nova, 17, 331-337.

Bouillin, J.P., Durand-Delga, M., Olivier, P.H., 1986. Betic-Rifian and Tyrrhenian Arcs: distinctive features, genesis and development stages. In: Wezel, F.C. (Ed.), The Origin of Arcs. Elsevier Science, Amsterdam, pp. 281–304.

Busquet, J.C., Gueremy, P., 1969. Quelques phénomènes de néotectonicque dans l'Apennin Calabro-Lucanien et leurs consequences morphologiques. II.-L'escarpment méridional du Pollino et son piémont. Revue de Géographie Physique et Géologie Dynamique, 11, 223-236.

Carobene, L., Damiani, A:V., 1985. Tettonica e sedimentazione pleistocenica nella media valle del fiume Crati. Area tra il torrente Pescara ed il fiume Mucone (Calabria). Bollettino della Società Geologica Italiana, 104, 115-127.

Catalano, R., Monaco, C., Tansi, C., 1993. Pleistocene strike-slip-tectonics in the Lucanian Apennine (Southern Italy). Tectonics, 12, 56–665.

Cello, G., Mazzoli, S., 1999. Apennine tectonics in southern Italy: a review. *Journal of* Geodynamics, 27, 191-211.

Cello, G., Tondi, E., Micarelli, L., Mattioni, L., 2003. Active tectonics and earthquake sources in the epicentral area of the 1857 Basilicata earthquake (Southern Italy). Journal of Geodynamics, 36, 37-50.

Chiarabba, C., De Gori, P., Speranza, F., 2008. The Southern Tyrrhenian Subduction Zone: Deep geometry, magmatism and Plio-Pleistocene evolution. Earth and Planetary Science Letters, 268, 408-423.

Cifelli, F., Rossetti, F., Mattei, M., 2006. The architecture of brittle postorogenic extension: Results from an integrated structural and paleomagnetic study in north Calabria (southern Italy). Geological Society American Bulletin, doi: 10.1130/B25900.1.

Colella, A., De Boer, P.L., Nisio, S.D., 1987. Sedimentology of a marine intermontane Pleistocene Gilbert-type fan delta complex in the Crati basin, Calabria, southern Italy. Sedimentology, 34, 721-736.

Colella, A. ,1988. Fault-controlled marine Gilbert-type fan deltas. Geology, 16, 1031-1034.

C.P.T.I. Working Group, 2004. Catalogo Parametrico Terremoti Italiani, 92 pp., Bologna.

Critelli, S., 1999. The interplay of lithosferic flexure and thrust accomodation in forming stratigrafic sequences in the Southern Appennines foreland basin sistem, Italy. Rendiconti Licei Scienze Fisiche e Naturali, Accademia Naturale dei Lincei, serie IX, vol. X(4).

Dewey, J.F., Helman, M.L., Turco, E., Hutton, D.H.W., Knott, S.D., 1989. Kinematics of the western Mediterranean. In: M.P. Coward, D. Dietrich and R.G. Park (eds) Alpine tectonics. Geological Society, London, Special Publication, 45, 265-283.

Di Nocera, S., Ortolani, F., Russo, B. Torre, M., 1974. Successioni sedimentarie Messiniane al limite Miocene-Pliocene nella Calabria settentrionale. Bollettino della Società Geologica Italiana, 93, 575-607.

Diss Working Group, 2009. Database of Individual Seismogenic Sources, a compilation of potential sources for earthquakes larger than M 5.5 in Italy and surrounding areas. Available at: http:// diss.rm.ingv.it/diss.

Doglioni, C., Merlini, S., Cantarella, G., 1999. Foredeep geometries at the front of the Apennines in the Ionian Sea (central Mediterranean). Earth and Planetary Letters 168, 243-254.

Ferranti, L., Santoro, E., Mazzella, M.E., Monaco, C., Morelli, D., 2009. Active transpression in the northern Calabria Apennines, southern Italy. Tectonophysics, 476, 226-251.

Ganas, A., Pavlides, S.B., Sboras, S., Valkaniotis, S.; Papaioannou, S., Alexandris, G.A., Plessa, A., Papadopoulos, G.A., 2004. Active fault geometry and kinematic in Parnitha Mountain, Attica, Greece. Journal of Structural Geology, 26, 2103-2118.

Ghisetti, F., Vezzani, L., 1982. Strutture tensionali e compressive indotti da meccanismi profondi lungo la linea del Pollino (Appennino meridionale). Bollettino della Società Geologica Italiana, 101, 385-440.

Goes, S., Giardini, D., Jenny, S. Hollenstein, C., Kahle, H.-G., Geiger A.., 2004. A recent tectonic reorganization in the south-central Mediterranean. Earth and Planetary Science Letters, 226, 335– 345.

Grandjacquet, C., Mascle, G. 1978. The structure of the Ionian sea-Sicily and Calabria-Lucania. In: Nairn, A.E.M., Kanes, H., Stehli, F.G. (Eds.), The Ocean Basins and Margins, vol. 5. Plenum Press, New York, pp. 257–329.

Guarnieri, P., 2006. Plio-Quaternary segmentation of the south Tyrrhenian forearc basin. International Journal of Earth Sciences, 107–118 DOI 10.1007/s00531-005-0005-2.

Iannace, A., Bonardi, G., D'Errico, M., Mazzoli, S., Perrone, V., Vitale, S. 2005. Structural settino and tectonic evolution of the Apennine Units of northern Calabria. Comptes Rendus Geoscience, 337, 1541-1550.

Johnston, S.T., Mazzoli, S., 2009. The Calabrian Orocline: buckling of a previously more linear orogen. In: Murphy, J. B., Keppie, J. D. and Hynes, A. J. (eds.) Ancient Orogens and Modern Analogues. Geological Society, London, Special Publications, 327, 113-125

Knott, S.D., Turco, E. 1991. Late Cenozoic kinematics of the Calabrian Arc, southern Italy. Tectonics, 10, 1164-1172.

Lanzafame, G., Zuffa, G.G., 1976. Geologia e petrografia del Foglio di Bisignano (Bacino del Crati, Calabria): Carta geologica alla scala 1:50000. Geologica Romana, 15, 223-270.

Lanzafame, G., Tortorici, L., 1981. La tettonica recente del Fiume Crati (Calabria). Geografia Fisica e Dinamica Quaternaria, 4, 11-21.

Malinverno, A., Ryan, W.B.F., 1986. Extension in the Tyrrhenian Sea and shortening in the Apennines as result of arc migration driven by sinking of the lithosphere. Tectonics, 5, 227-245.

Mattei, M., Cipollari, P., Cosentino, D., Argentieri, A., Rossetti, F., Speranza, F., Di Bella, L., 2002. The Miocene tectono-sedimentary evolution of the Southern Tyrrhenian Sea: stratigraphy, structural and paleomagnetic data from the onshore Amantea basin (Calabrian Arc, Italy). Basin Research, 14, 147-168.

Mattei, M., Cifelli, F., D'Agostino, N., 2007. The evolution of the Calabrian Arc: Evidence from paleomagnetic and GPS observations. Earth and Planetary Science Letters, 263, 3-4, 259-274.

Mazzoli, S., Helman, M., 1994. Neogene patterns of relative plate motion for Africa–Europe: some implications for recent central Mediterranean tectonics. Geologische Rundschau, 83, 464–468.

Milia, A., Turco, E., Pierantoni, P.P., Schettino, A.., 2009. Faour-dimensional tectono-stratigraphic evolution of the southeastern peri-Tyrrhenian Basins (Margin of Calabria, Italy). Tectonophysics, 476, 41-56.

Monaco, C., Tortorici, L., 2000. Active faulting in the Calabrian Arc and eastern Sicily. Journal of Geodynamics, 29, 407–424.

Monaco, C., Tortorici, L., Nicolich, R., Cernobori, L., Costa, M., 1996. From collisional to rifted basins: an example from the southern Calabrian Arc (Italy). Tectonophysics, 266, 233–249.

Muto, F., Perri, E. 2002. Evoluzione tettono-sedimentaria del bacino di Amantea, Calabria occidentale. Bollettino della Società Geologica Italiana, 121, 391-409.

Ogniben, L., 1973. Schema geologico della Calabria in base ai dati odierni. Geologica Romana, 12, 243-585.

Ortolani, F., Pagliuca, S., Pepe, E., Schiattarella, M., Toccaceli, R. M., 1992. Active tectonics in the southern Apennines: relationships between cover geometries and basement structure. A hypotesis for geodynamic model. IGCP 276, Newsletters, 5, 413-419.

Pepe, F., Sulli, A., Bertotti, G., Cella, F. The architecture and Neogene to Recent evolution of the W Calabrian continental margin: an upper plate perspective to the Ionian subduction system (Central Mediterranean). Tectonics, *in press*.

Perri, E. 1997. Tettonica post-tortoniana del settore nord-occidentale dell'Arco Calabro. Studi Geologici Camerti, 14, 155-175.

Perri, E., Schiattarella, M., 1997. Evoluzione tettonica quaternaria del bacino di Morano Calabro (Catena del Pollino, Calabria settentrionale). Bollettino della Società Geologica Italiana, 116, 3-15.

Petit, C., Meyer, B., Gunnell, Y., Jolivet, M., Sankov, V., Strak, V., Gonga-Saholiariliva, N. The height of faceted spurs, a proxy for determining long-term throw rates on normal faults: evidence from the North Baikal Rift System, Siberia. Tectonics, *In press*.

Piccardi, L., Gauderner, Y., Tapponier, P., Boccaletti, M., 1999. Active oblique extension in the central Apennines (Italy): evidence from the Fucino region. Geophysical Journal International, 139, 499-530.

Pizzi, A., Galadini, F., 2009. Pre-existing cross-structures and active fault segmentation in the northern-central Apennines (Italy). Tectonophysics, 476, 304-319.

Reches, Z., 1987. Determination of the tectonic stress tensor from slip along faults that obey the Coulomb yield condition. Tectonics, 6, 849-861.

Rio, D., Sprovieri, R., Thunell, R., 1991. Pliocene-Lower Pleistocene chronostratigraphy: a re-evaluation of Mediterranean type sections. American Bulletin of the Geological Society, 103, 1049-1058.

Roberts, G.P., Ganas, A., 1996. Fault-slip directions in central-southern Greece measured from striated and corrugated fault planes: comparison with focal mechanism and geodetic data. Journal of Geophysical Research, 105, 443-462.

Roberts, G.P., Cowie, P., Papanikolaou, I., Michetti, A.M., 2004. Fault scaling relationships, deformation rates and seismic hazard: an example from the Lazio-Abruzzo Appennines, central Italy. Journal of Structural Geology, 26, 377-398.

Romeo, M., Tortorici, L., 1980. Stratigrafia dei depositi miocenici della Catena Costiera calabra meridionale e della media Valle del F. Crati (Calabria). Bollettino della Società Geologica Italiana, 99, 302-318.

Rossetti, F., Faccenna, C., Goffè, B.; Monié, P., Argentieri, A., Funiciello, R., Mattei, M., 2001. Alpine structural and metamorphic segnature of the Sila Piccola Massif nappe stack (Calabria, Italy): Insights for the tectonic evolution of the Calabrian Arc. Tectonics, 20, 112-133.

Russo, F., Schiattarella, M., 1992. Osservazioni preliminari sull'evoluzione morfostrutturale del bacino di Castrovillari (Calabria settentrionale). Studi Geologici Camerti, Special Issue 1, 271-278.

Sartori, R., 1989. Evoluzione neogenico-recente del bacino tirrenico e suoi rapporti con la geologia delle aree circostanti. Giornale di Geologia, 51, 1-39.

Sartori, R., 1990. The main results of ODP LEG 107 in frame of Neogene to recent geology of peri-tyrrhenian areas. Proceeding of the Ocean Drilling Program, Scientific Results, 107, 715-730.

Scandone, P., 1979. Origin of the Tyrrhenian Sea and Calabrian Arc. Bollettino della Società Geologica Italiana, 98, 27-34.

Schiattarella, M., 1996. Tettonica della Catena del Pollino (confine Calabro-Lucano). Memorie della Società Geologica Italiana, 51, 543-566.

Schiattarella, M., 1998. Quaternary tectonics of the Pollino Ridge, Calabria-Lucania boundary, southern Italy. In: R.E., Holdsworth, R:A., Strachan and J.F.Dewey (eds) Continental Transpressional and Transtensional Tectonics. Geological Society, London, Special Publication, 135, 341-354.

Scholz, C.H., Gupta A.., 2000. Fault interactions and seismic hazard. *Journal of* Geodynamics, 29, 459-467.

Spina, V., Tondi, E., Galli. P., Mazzoli, S., Cello, G., 2008. Quaternary fault segmentation and interaction in the epicentral area of the 1561 earthquake (Mw = 6.4), Vallo di Diano, southern Apennines, Italy. Tectonophysics, 453, 233-245.

Spina, V., Tondi, E., Galli, P., Mazzoli, S., 2009. Fault propagation in a seismic gap area (northern Calabria, Italy): Implication for seismic hazard. Tectonophysics, 476, 357-369.

Sprovieri, R., 1992. Mediterranean Pliocene biochronology: an high resolution record based on quantitative planktonic foraminifera distribution. Rivista Italiana di Paleontologia e Stratigrafia, 98, 1, 61-100.

Tansi, C., Tallarico, A., Iovine, G., Folino Gallo, M., Falcone, G., 2005. Interpretation of radon anomalies in seismotectonic and tectonic-gravitational settings: the south-eastern Crati graben (Northern Calabria, Italy). Tectonophysics, 396, 181-193.

Tansi, C., Muto, F., Critelli, S., Iovine, G. 2007. Neogene-Quaternary strike-slip tectonics in the central Calabrian Arc (southern Italy). Journal of Geodynamics, 43, 393-414.

Thomson, S. N., 1994. Fission track analysis of the crystalline basement rocks of the Oligo-Miocene late-orogenic extension and erosion. Tectonophysics, 238, 331–352.

Tondi, E., 2000. Geological analysis and seismic hazard in the Central Apennines. Journal of Geodynamics, 29, 517-534.

Tondi, E., Cello, G., 2003. Spatiotemporal Evolution of the Central Apennines Fault System (Italy). Journal of Geodynamics, 36, 113-128.

Tortorici, L., 1981. Analisi delle deformazioni fragili dei sedimenti postorogenici della Calabria settentrionale. Bollettino della Società Geologica Italiana, 100, 291-308.

Tortorici, L., 1982. Lineamenti geologico-strutturali dell'Arco Calabro. Società Italiana di Mineralogia e Petrologia, 38, 927–940.

Tortorici, L., Monaco, C., Tansi C., Cocina, O., 1995. Recent and active tectonics in the Calabrian arc (Southern Italy). Tectonophysics, 234, 37-55.

Trincardi, F., Zitellini, N., 1987. The rifting of the Tyrrhenian Basin. Geomarine Letters, 7, 1-6

Turco, E., Maresca, R., Cappadona, P., 1990. La tettonica plio-pleistocenica del confine calabro-lucano: modello cinematico. Memorie della Società Geologica Italiana, 45, 519-529.

Van Dijk, J.P., Bello, M., Brancaleoni, G.P., Cantarella, G., Costa, V., Frixa, A., Golfetto, F., Merlini, S., Riva, M., Torricelli, S., Toscano, C., Zerilli A., 2000. A regional structural model for the northern sector of the Calabrian Arc (southern Italy). Tectonophysics, 324, 267-320.

Vezzani, L., 1968. I terreni plio-pleistocenici del basso Crati (Cosenza). Atti dell'Accademia Gioenia di Scienze Naturali di Catania, 6, 28-84.

Westaway, R., 1993. Quaternary uplift of southern Italy. Journal of Geophysical Research, 98, 21741-21722.

Wortel, M.J.R., Spackman, W., 1993. The dynamic evolution of the Apenninic-Calabrian, Hellenic and Carpathian arcs: a unifying approach. Terra Nova Abstract, 1,5, 97.

Xiaohan, L., 1983. Perturbation de contraintes liées aux structures cassantes dans les calcaires fins du Languedoc. Observations et simulations mathématiques (Stress field perturbation induced by brittle structures in the Languedoc limestone. Observation and mathematical simulations). Ph.D. Thesis University of Montpellier, Montpellier.

FIGURE CAPTIONS

Fig.1. (a) Digital elevation model showing main strike-slip faults and extensional basins of the southern Apennines and northern Calabria. Major strike-slip fault zones (*sensu* Van Dijk et al., 2000, Tansi et al., 2007): Pollino Fault Zone (PFZ), Petilia-S.Sosti Fault Zone (PSSFZ), Falconara-Cosenza Fault Zone (FCFZ), Amantea-Gimigliano Fault Zone (AGFZ), S.Nicola-Rossano Fault Zone (SRFZ). (b) Geological sketch map of northern Calabria. (c) Topographic section across the Crati Basin, the Coastal Range and the Sila Massif.

Fig. 2. (a) Chrono-stratigraphic section and (b) E-W oriented chrono-stratigraphic framework of the Crati Basin. In the peripheral areas of the basin, sedimentary intervals are characterized by erosional contacts and angular unconformities evolving to para-concordant boundaries towards the main basin depocentre. (c) Lithostratigraphic logs showing the distribution of the different stratigraphic formations and their relationships as observed in the southern sector of the basin.

Fig. 3. Geological maps of the Crati Basin. (a) Northern border area of the basin (Pollino area). (b) Southern and central sectors of the basin.

Fig. 4. Field examples of contractional and strike-slip structures affecting the basin infill (see Fig. 3 for location). (a) Overturned fold showing NNW trending axis and sub-horizontal axial surface involving arenites of the first Pliocene sub-synthem (1 Ps). (b) Minor reverse fault (showing approximately 1 m of displacement) within Lower Pleistocene conglomerates. (c) High-angle reverse fault between Lower Pleistocene fan conglomerates

and Mesozoic carbonates. (d) Left-lateral strike-slip fault cutting Pleistocene deposits along the Pollino foothills.

Fig. 5. Field examples of extensional structures affecting the Crati Basin (see Fig. 3 for location). (a) 3D view of the western border of the basin. N-S striking, left-stepping normal faults (marked by a series of facet spurs) border the Crati Basin. The Montalto Uffugo-Rende Fault (MRF) abuts against the NW-SE striking, left-lateral, Falconara-Cosenza Fault Zone (FCFZ, represented by thick blue lines in b). (c) Normal faults affecting Lower-Middle Pleistocene conglomerates in the depocentral zone of the basin. The faults are marked by rotated and aligned pebbles (detail in inset d). Fault planes are sealed by deposits of the same formation (thick dotted line), suggesting that the faults are syn-sedimentary. (e) Lower-Middle Pleistocene growth strata associated with normal fault activity. (f) 3D view of the northernmost sector of the Crati Basin. A series of overstepping fault scarps show an elliptical profile, strongly decreasing towards the impressive fault wall along the Pollino Range. (g) Detail of the fault scarp shown in (e): faults affect Middle Pleistocene breccias and exhibit oblique normal left-lateral kinematics.

Fig. 6. Evidence of normal faulting along the eastern margin of the Crati Basin (see Fig. 3 for location). (a) Normal fault plane exposed in crystalline bedrock, also offsetting Lower Pleistocene sands and conglomerates. (b) Striated fault plane in bedrock in the same locality. Structural data indicate dominant extensional kinematics with a left-lateral component of motion. (c) High angle ~N-S striking faults downthrowing well bedded fossiliferous sands with respect to the basal conglomerates and coarse-grained sediments onlapping the crystalline basement.

Fig. 7. (a) Structural data for the southern and central sectors and (b) for the northernmost part of the Crati Basin. Rose diagrams display the main fault trends. Contour diagrams show the distribution of the striae measured along fault planes, with results of kinematic data inversion for palaeostress analysis. Symbols represent the stress values (σ1 maximum and σ3 minimum), white arrows show maximum extension directions. Histograms show accuracy of the data.

Fig. 8. Correlations of deep wells in the Sibari Plain.

Fig. 9. Velocity (Vp) vs. depth for Thurio-1 and Ogliastrello wells. These data have been used to estimate average velocity values for different stratigraphic units.

Fig. 10. Interpreted 2D seismic lines available for the study area.

Fig. 11. (a) 3D view of Calabria showing rough distribution of macroseismic areas for M>5 earthquakes (from diss Working Group, 2009). Red lines represent active faults (numbers indicate faults labeled in b); blue lines represent regional strike-slip fault zones affecting the western sector of northern Calabria (as shown in Fig. 1). (b) Digital terrain model showing details of the major seismic events (M>5) that occurred in the western sector of Calabria during historical times (from CPTI, 2004). Both instrumental and historical seismicity cluster along major normal faults; such structures are segmented by basement-involving strike-slip fault zones (thick dotted lines). Thick arrows show maximum extension direction (direction of the minimum compressive stress axis σ3) characterizing the major basins of the

Calabrian back-arc region (i.e. Crati and Mesima basins). Active normal faults form the Siculo-Calabra Rift Zone (*sensu* Monaco and Tortorici, 2000), which is thought to be an actively extending sector (red areas in the figure) within the inner (i.e. western) portion of the Calabrian belt.

Fig. 12. Evolution of the Crati Basin and the western sector of northern Calabria (see text for details). Tectonic sketches (in red structures active at different times) are coupled with the related stratigraphic columns: blue areas represent exposed landmass undergoing erosional processes and supplying sediments to both the Tyrrhenian and the Ionian basins. White arrows indicate stress type and approximate orientation for Tyrrhenian off-shore and the Crati Basin. Pollino Fault Zone (PFZ); Petilia-San Sosti Fault Zone (PSSFZ); Falconara-Cosenza Fault Zone (FCFZ); Amantea-Gimigliano Fault Zone (AGFZ).
(a). Sketch showing depocentres and tectonic structures active up to the Late Miocene. The 3D view of the western side of the Coastal Range shows the main attitude of the Late Miocene deposits (tilted towards the west), as well as the tectonic contacts between different basement units. W-dipping normal faults offset the original geological contacts. Bedding attitude, coupled with further geological evidence, confirm that this side of the Coastal Range is coincident with the limb of a regional anticline. (b) Sketch showing structures active up to the Middle-Upper Pliocene. (c) Sketch showing structures active up to the Middle Pleistocene. (d) Sketch showing the main sedimentary accumulations and tectonic structures active since Late Pleistocene time. (e) 3D view showing the relationships, at the regional scale, between the Paola Basin, the Coastal Range anticline and the Crati Basin.

Fig. 13. Time-space propagation of extension within the Crati Basin from Middle Pleistocene to Holocene times. Normal faults have formed in the southern part of the basin

since the Middle Pleistocene, abutting against the Falconara-Cosenza Fault Zone (FCFZ), and then propagated northwards. During the Late Pleistocene-Holocene, normal faults formed also in the northernmost sector of the basin, where the Pollino Fault Zone (PFZ) was partially re-activated in extension (see also Spina et al., 2009).

Table 1. Results of biostratigraphic analyses (planktonic foraminifera) on marine clays sampled in the southern sector of the Crati Basin (see Fig. 3 B for location). The appearance of *Hyalinea baltica* in the sections 4, 5 and 6, is widely recognized as indicative of the Lower Pleistocene (Rio et al., 1991).

Age of clays sampled in the sections 3, 4 and 5 has been estimated by Stigliano D. and Tripodi A.

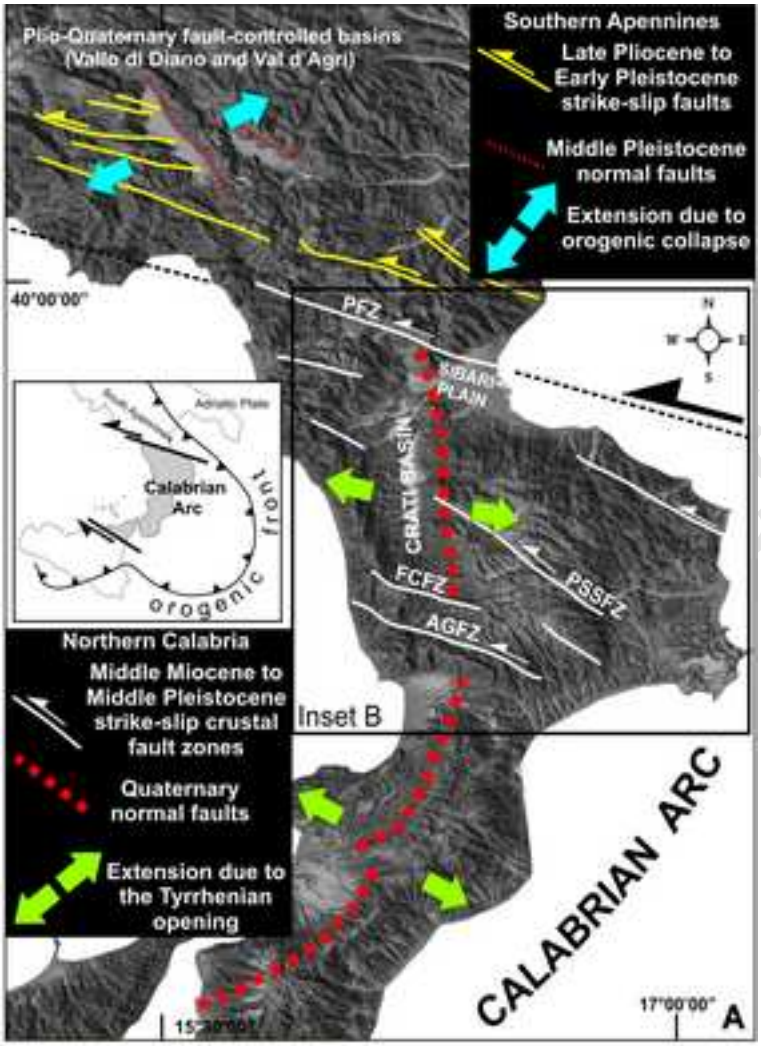

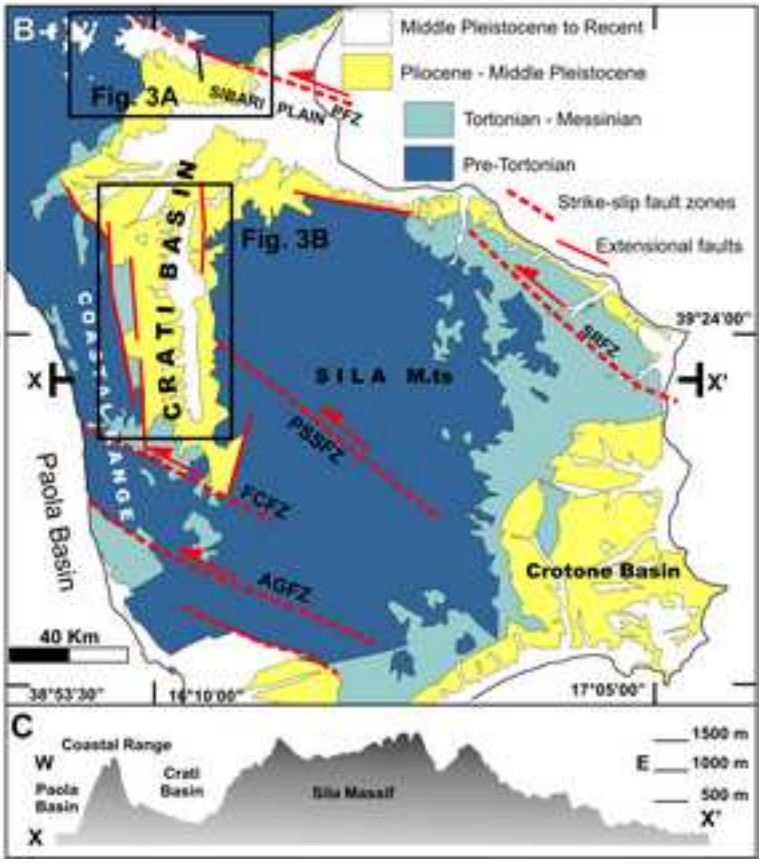

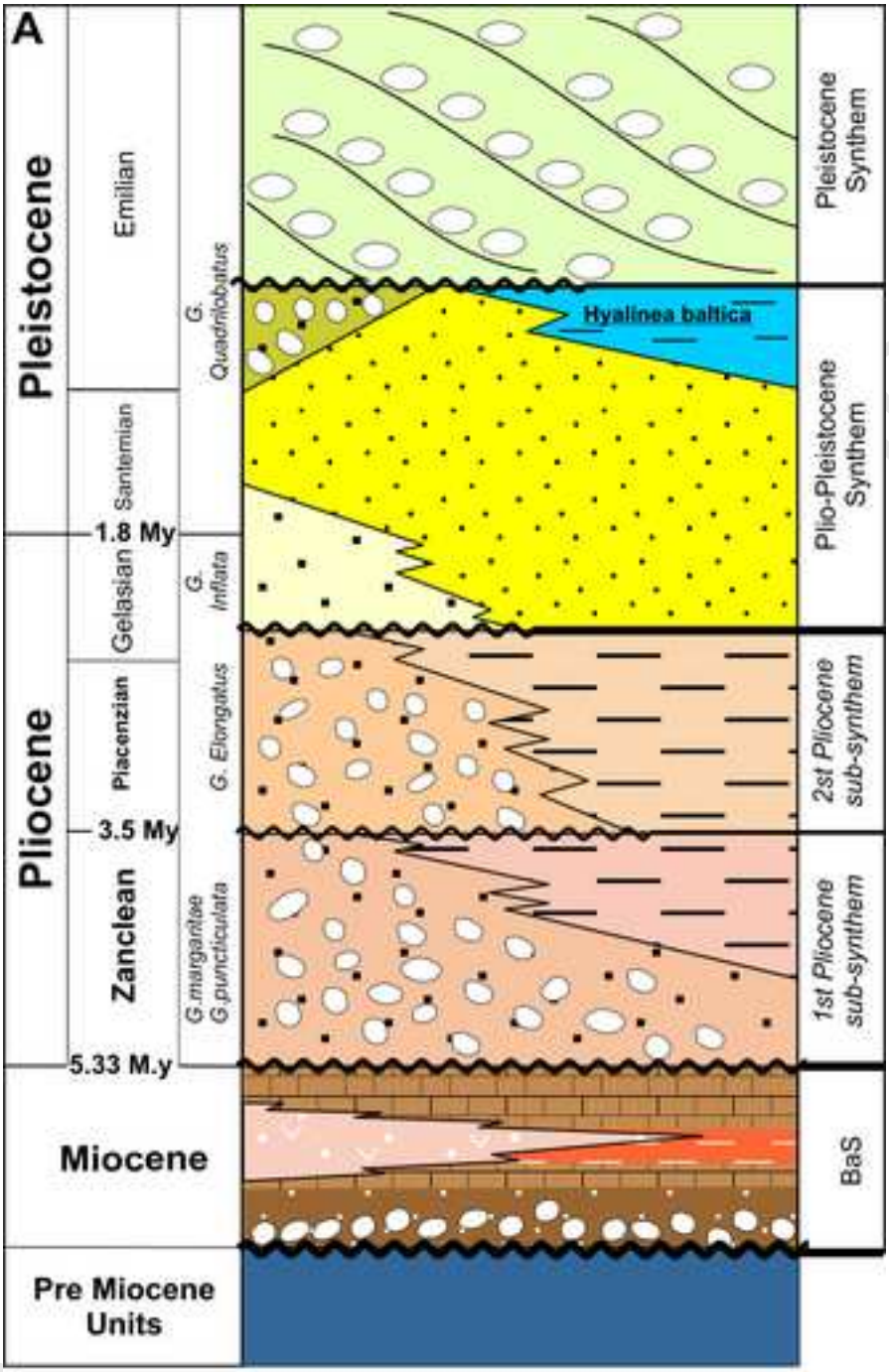

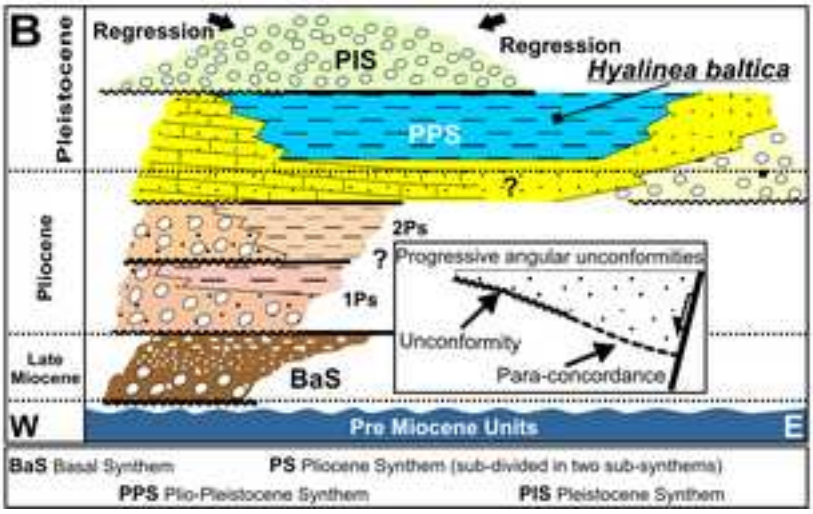

Figure

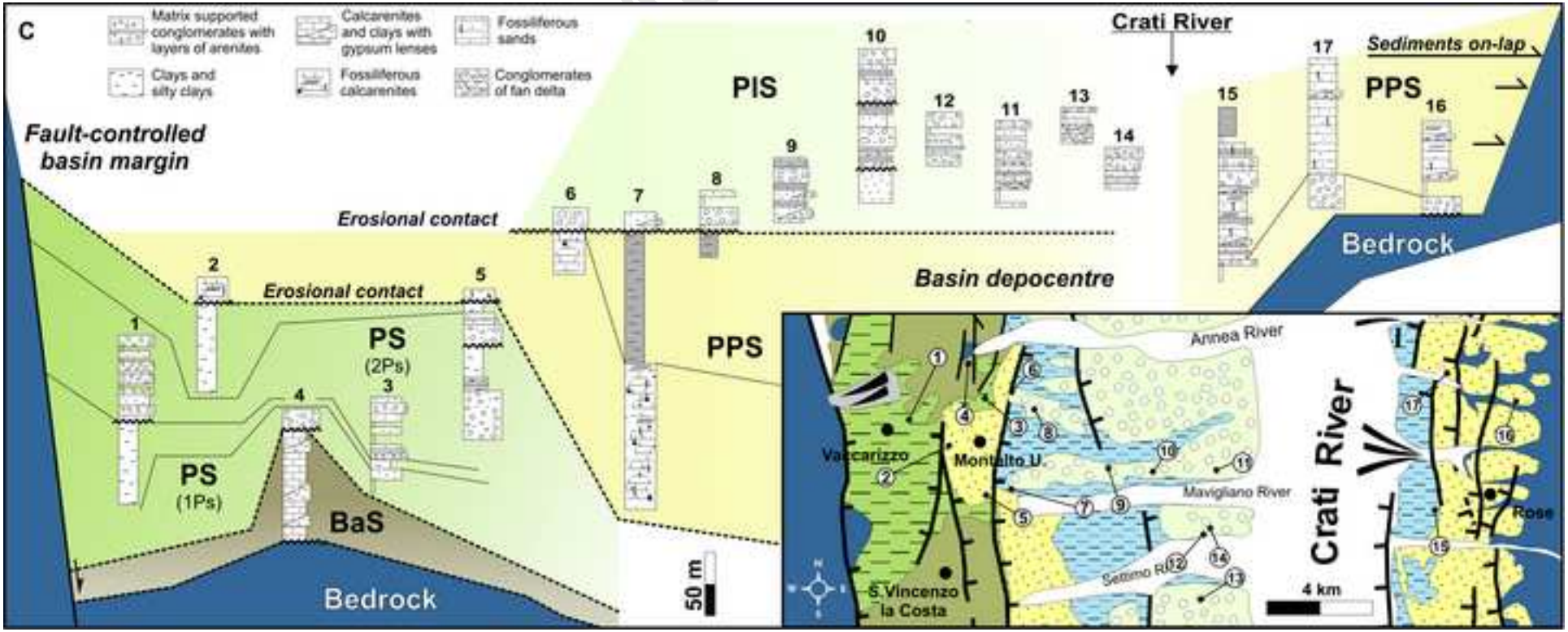
C
Matrix supported conglomerates with layers of arenites
Calcarenites and clays with gypsum lenses
Fossiliferous sands
Clays and silty clays
Fossiliferous calcarenites
Conglomerates of fan delta
Fault-controlled basin margin
PIS
Crati River
Sediments on-lap
PPS
Erosional contact
Basin depocentre
Bedrock
Erosional contact
PS
(2Ps)
PS
(1Ps)
BaS
PPS
Bedrock
50 m
Annea River
Vaccarizzo
Montalto U.
Mavigliano River
Crati River
Rose
Settimo R.
S.Vincenzo la Costa
4 km

Figure

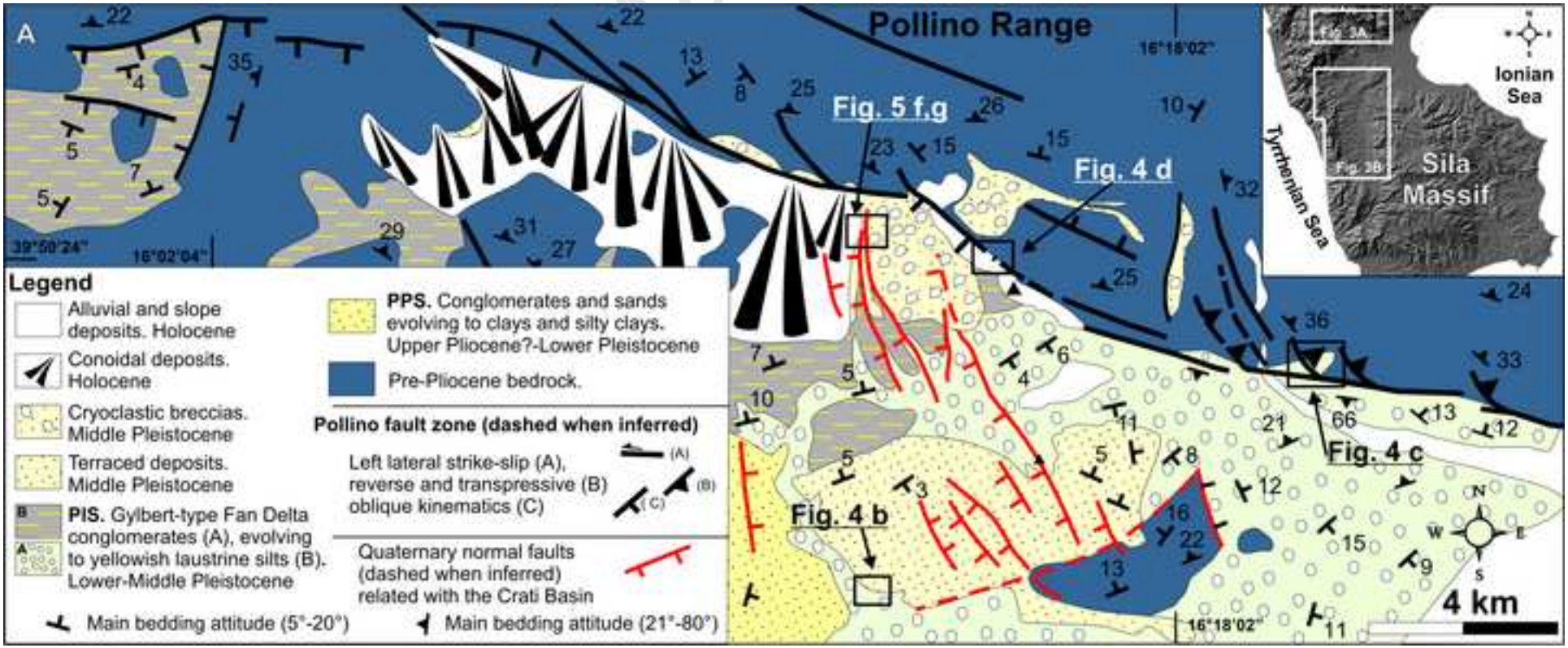
A
Pollino Range
Fig. 5 f,g
Fig. 4 d
Fig. 4 b
Fig. 4 c
Fig. 3A
Fig. 3B
Ionian Sea
Tyrrhenian Sea
Sila Massif
39°59'24"
16°02'04"
16°18'02"
4 km
Legend
Alluvial and slope deposits. Holocene
Conoidal deposits. Holocene
Cryoclastic breccias. Middle Pleistocene
Terraced deposits. Middle Pleistocene
PIS. Gylbert-type Fan Delta conglomerates (A), evolving to yellowish laustrine silts (B). Lower-Middle Pleistocene
PPS. Conglomerates and sands evolving to clays and silty clays. Upper Pliocene?-Lower Pleistocene
Pre-Pliocene bedrock.
Pollino fault zone (dashed when inferred)
Left lateral strike-slip (A), reverse and transpressive (B) oblique kinematics (C)
Quaternary normal faults (dashed when inferred) related with the Crati Basin
Main bedding attitude (5°-20°)
Main bedding attitude (21°-80°)

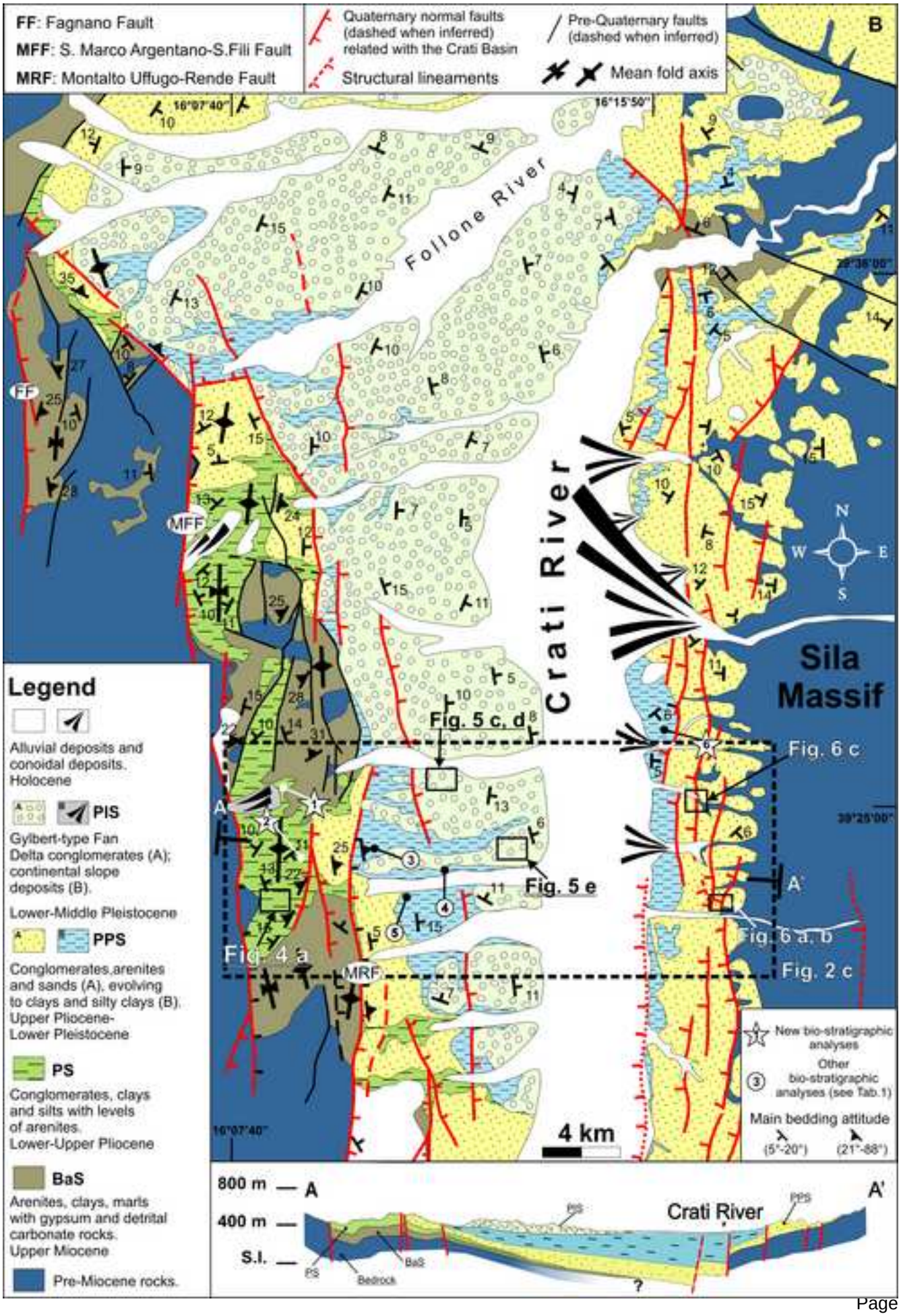

Figure

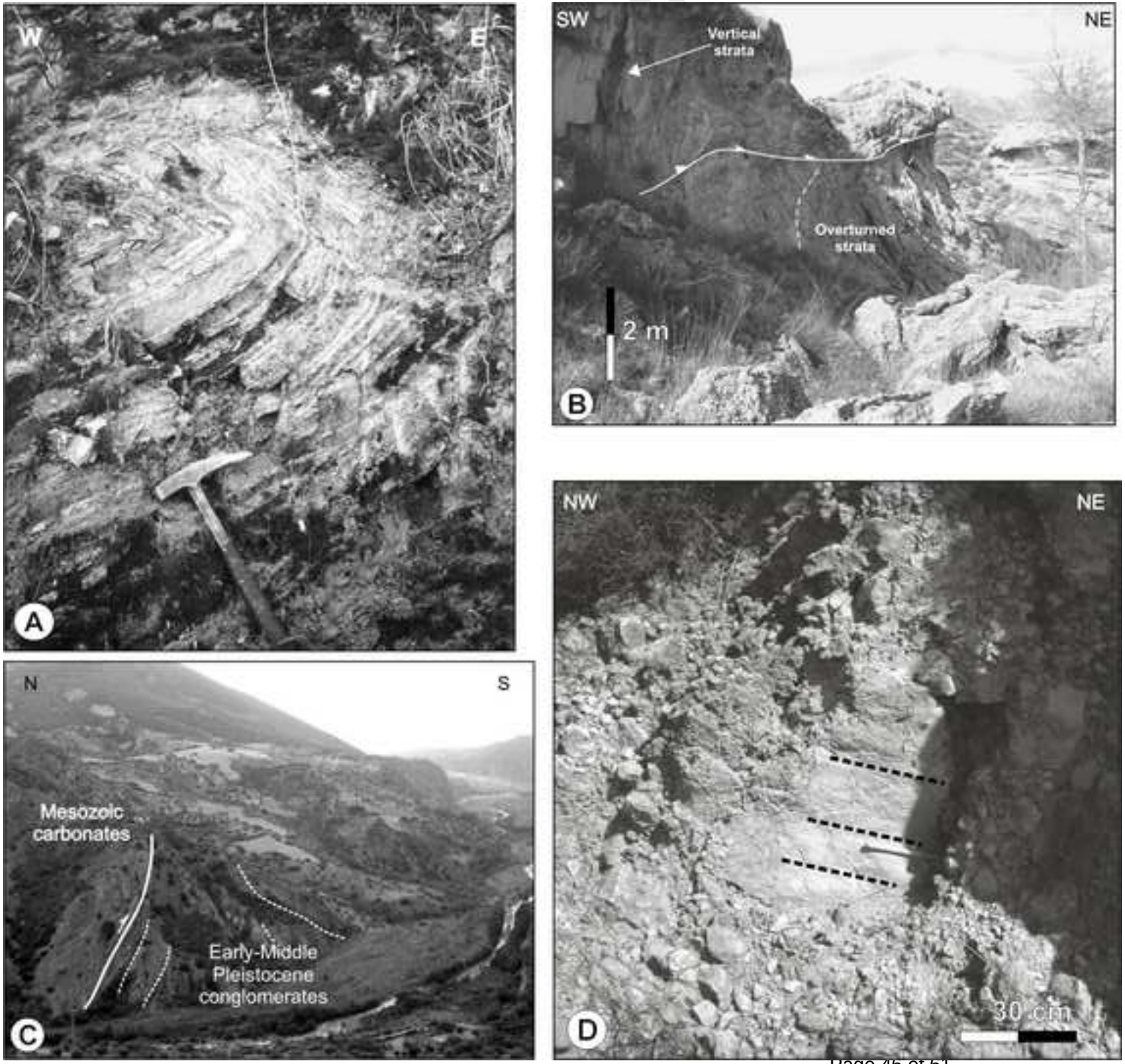
W
E
A
SW
NE
Vertical strata
Overturned strata
2 m
B
NW
NE
30 cm
D
N
S
Mesozoic carbonates
Early-Middle Pleistocene conglomerates
C

Figure

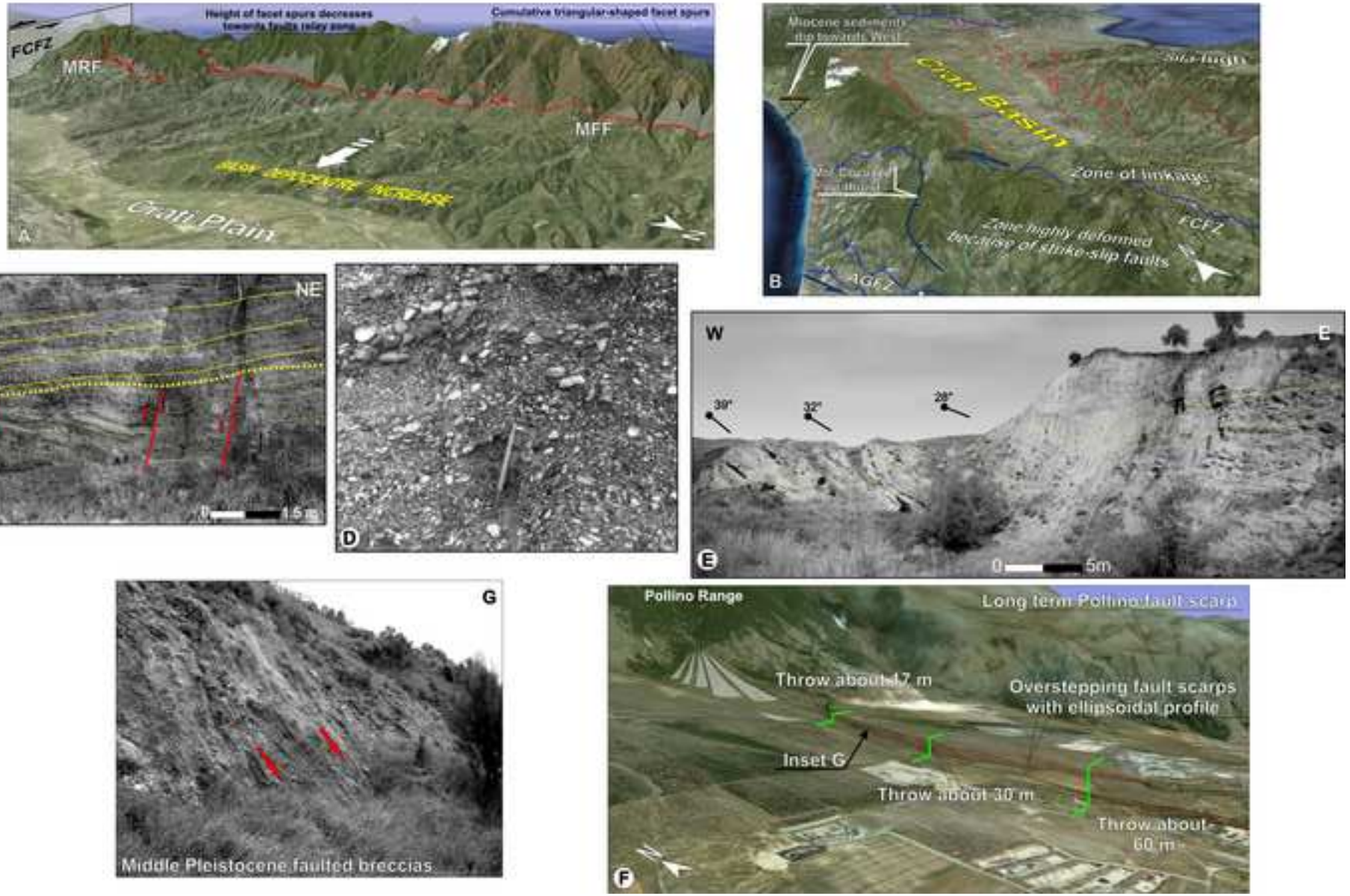
Height of facet spurs decreases towards faults relay zone
Cumulative triangular-shaped facet spurs
FCFZ
MRF
MFF
Fault Plain
A
Miocene sediments dip towards West
Crati Basin
Zone of linkage
Zone highly deformed because of strike-slip faults
FCFZ
AGFZ
B
SW
NE
D
C
1.5 m
D
W
E
39°
32°
28°
E
0
5m
G
Middle Pleistocene faulted breccias
Pollino Range
Long term Pollino fault scarp
Throw about 47 m
Overstepping fault scarps with ellipsoidal profile
Inset G
Throw about 30 m
Throw about 60 m
F

Figure

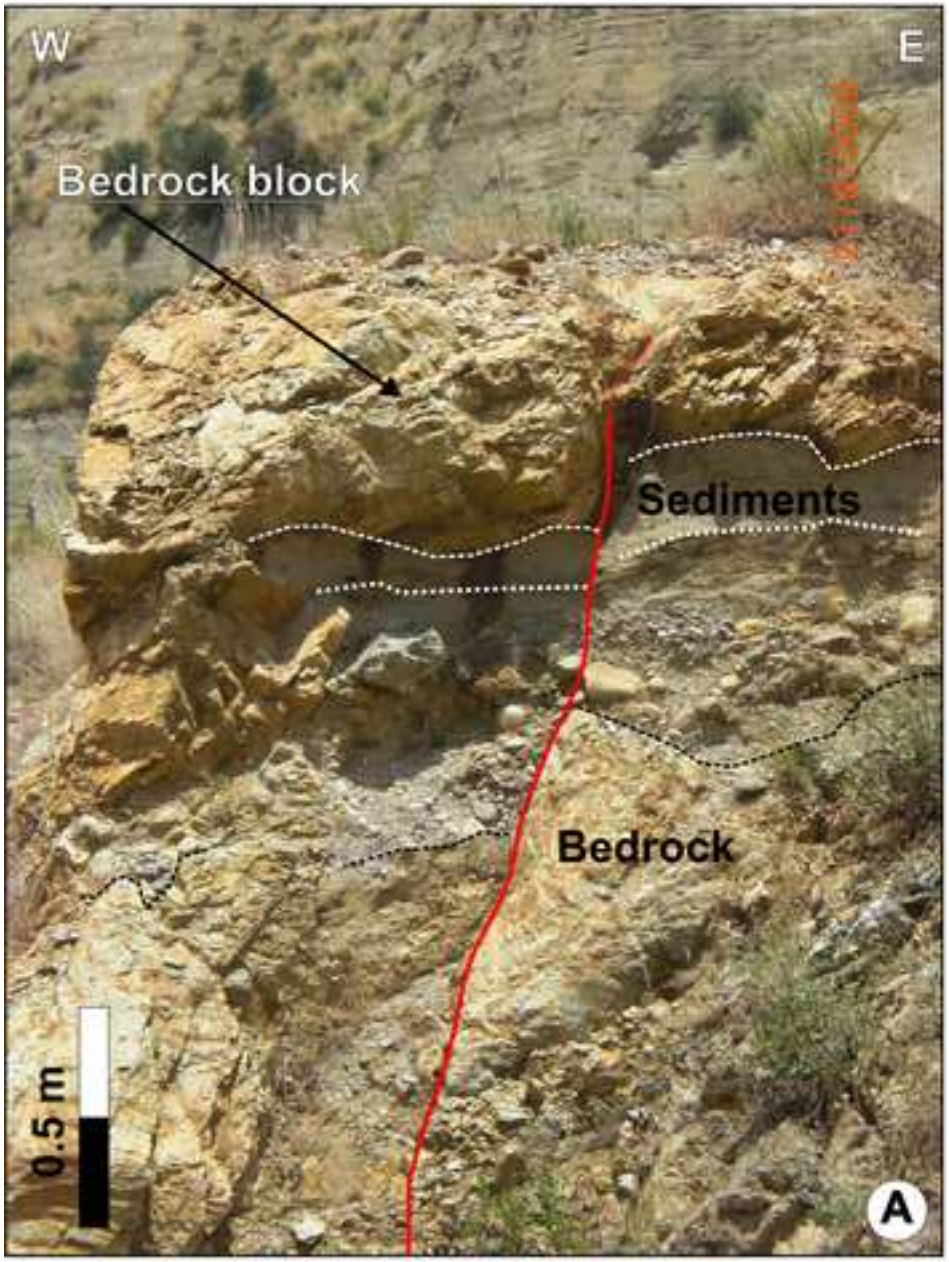
W
E
Bedrock block
Sediments
Bedrock
0.5 m
A

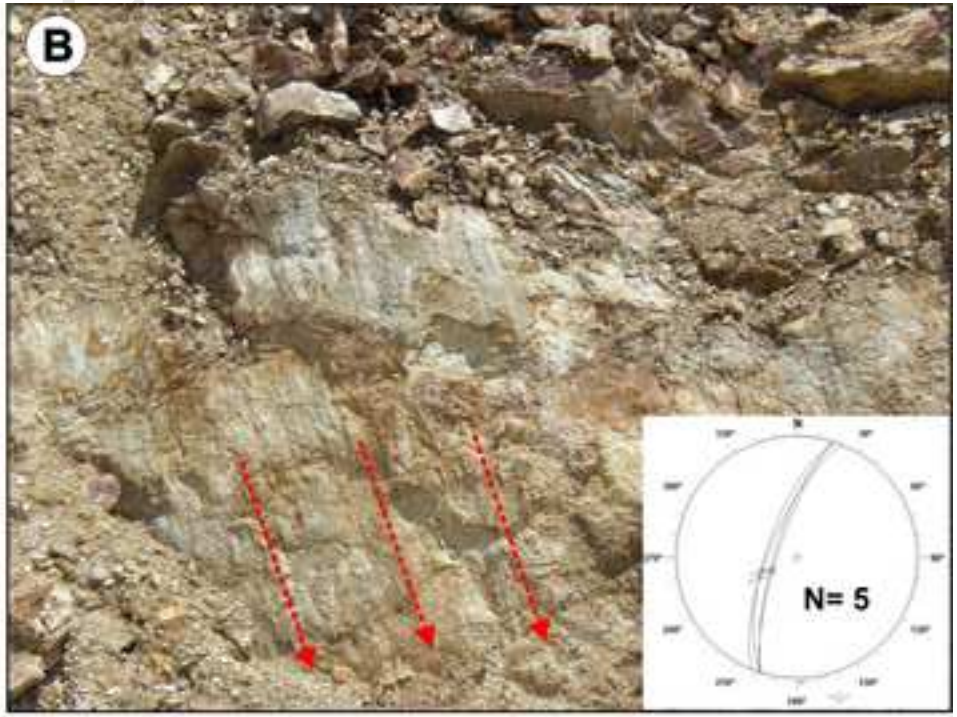
B
N= 5

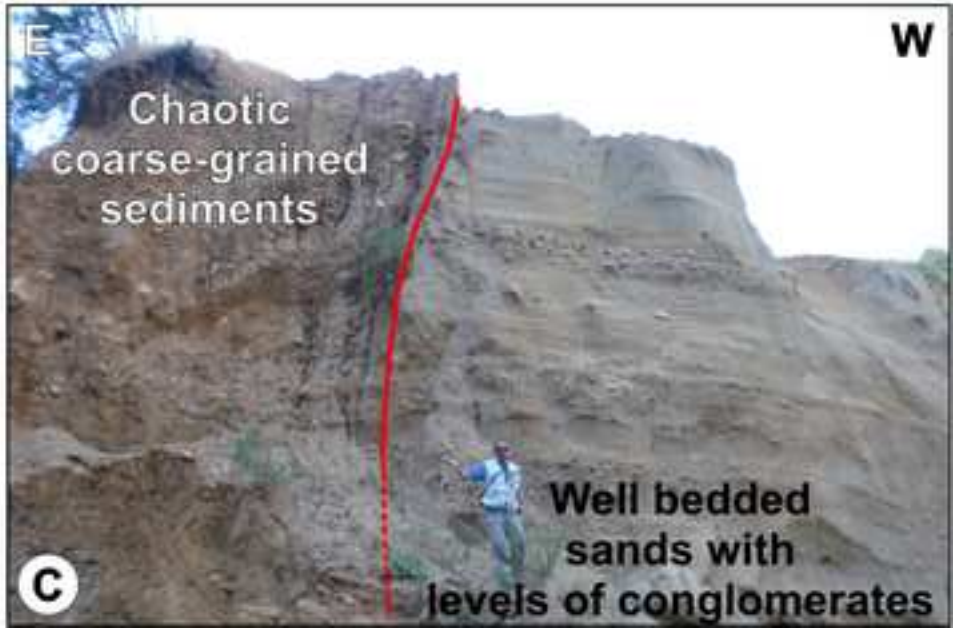
E
W
Chaotic coarse-grained sediments
Well bedded sands with levels of conglomerates
C

Figure

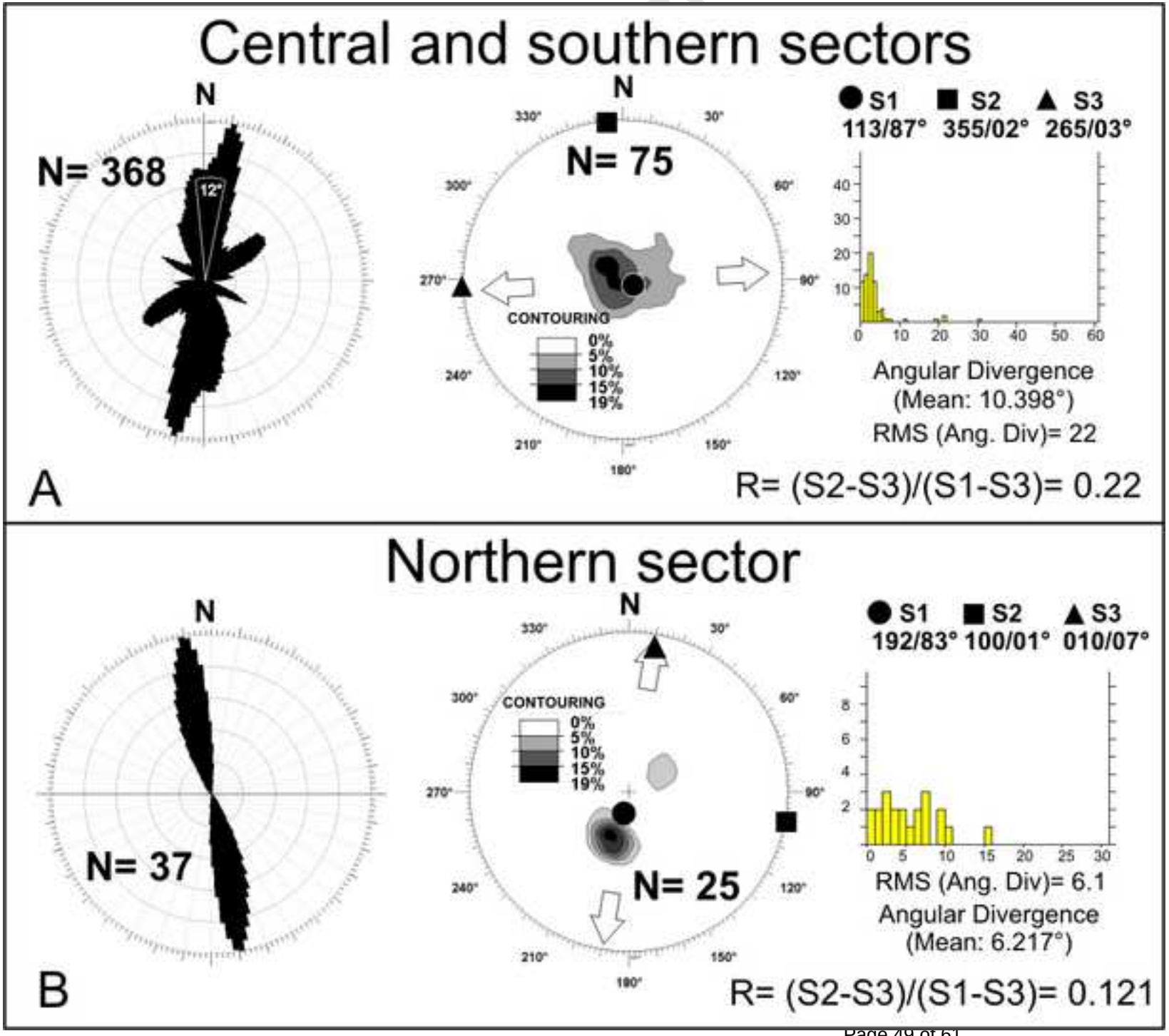
Central and southern sectors
N
N= 368
12°
N
N= 75
330°
30°
300°
60°
270°
90°
240°
120°
210°
150°
180°
CONTOURING
0%
5%
10%
15%
19%
S1 S2 S3
113/87° 355/02° 265/03°
40
30
20
10
0 10 20 30 40 50 60
Angular Divergence
(Mean: 10.398°)
RMS (Ang. Div)= 22
A
R= (S2-S3)/(S1-S3)= 0.22
Northern sector
N
N= 37
N
CONTOURING
0%
5%
10%
15%
19%
N= 25
S1 S2 S3
192/83° 100/01° 010/07°
8
6
4
2
0 5 10 15 20 25 30
RMS (Ang. Div)= 6.1
Angular Divergence
(Mean: 6.217°)
B
R= (S2-S3)/(S1-S3)= 0.121

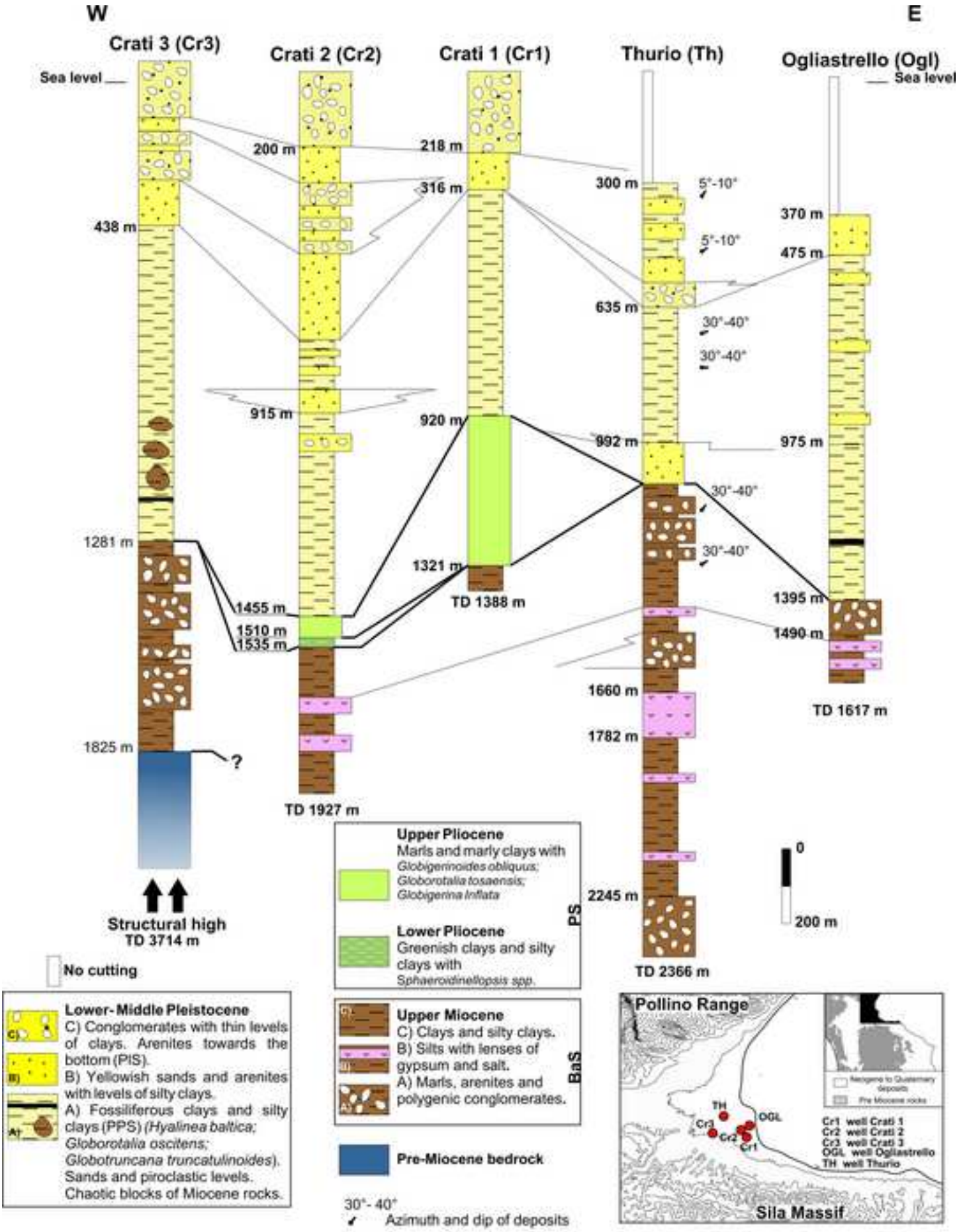

Figure

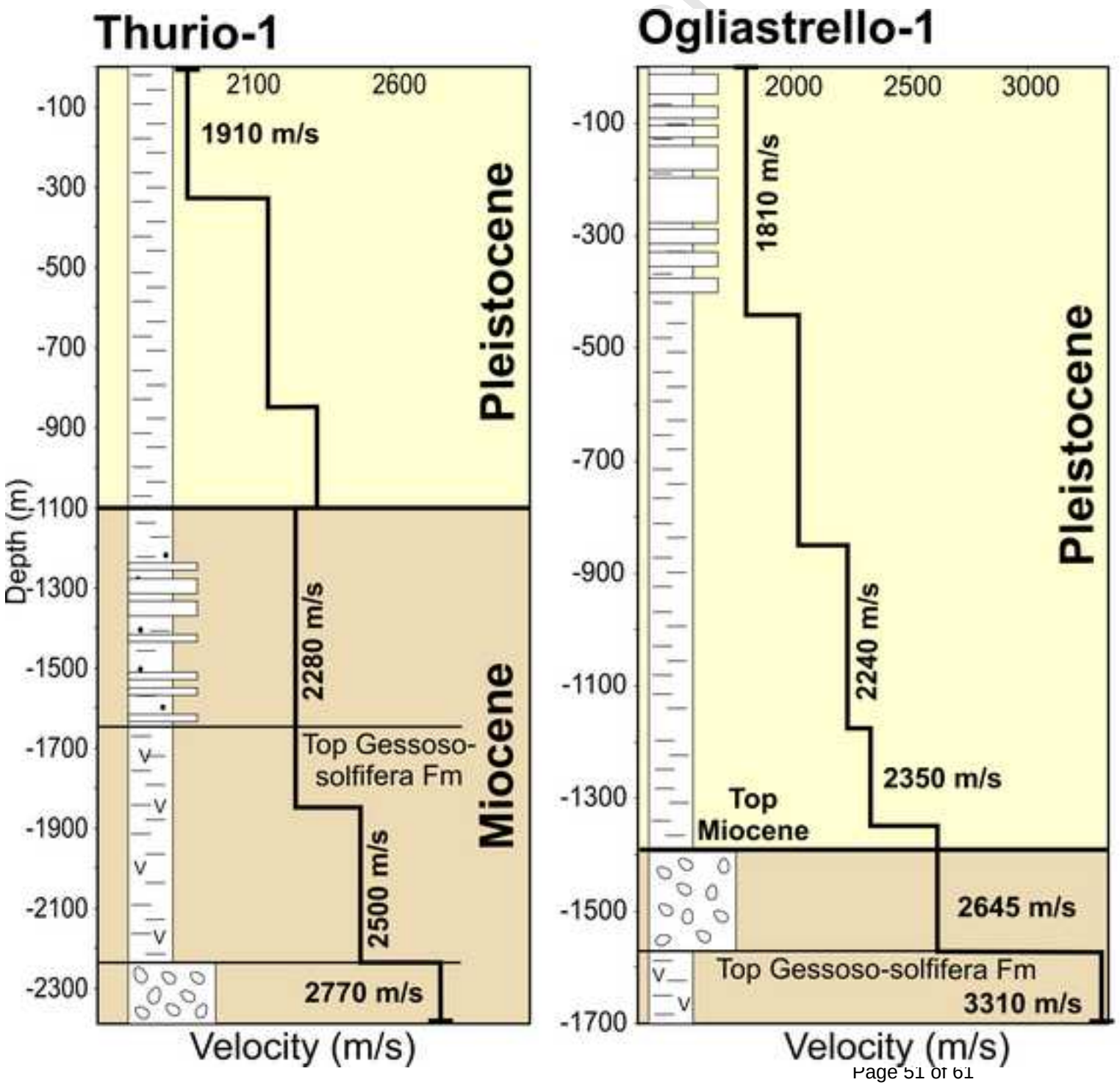
Thurio-1
2100
2600
1910 m/s
Pleistocene
2280 m/s
Top Gessoso-solfifera Fm
Miocene
2500 m/s
2770 m/s
Depth (m)
-100
-300
-500
-700
-900
-1100
-1300
-1500
-1700
-1900
-2100
-2300
Velocity (m/s)
Ogliastrello-1
2000
2500
3000
1810 m/s
Pleistocene
2240 m/s
2350 m/s
Top Miocene
2645 m/s
Top Gessoso-solfifera Fm
3310 m/s
-100
-300
-500
-700
-900
-1100
-1300
-1500
-1700
Velocity (m/s)

Figure

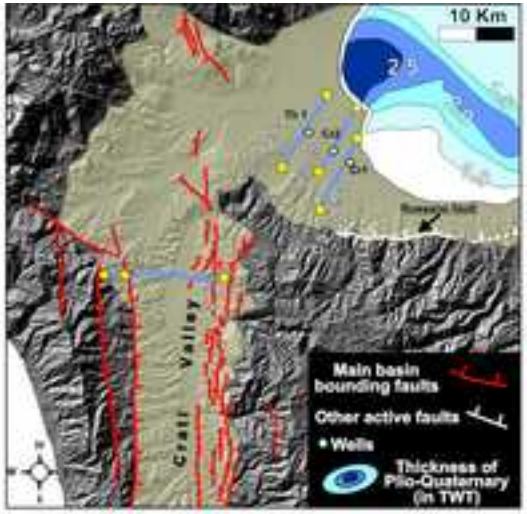
10 Km
Crati Valley
Main basin bounding faults
Other active faults
Wells
Thickness of Plio-Quaternary (in TWT)

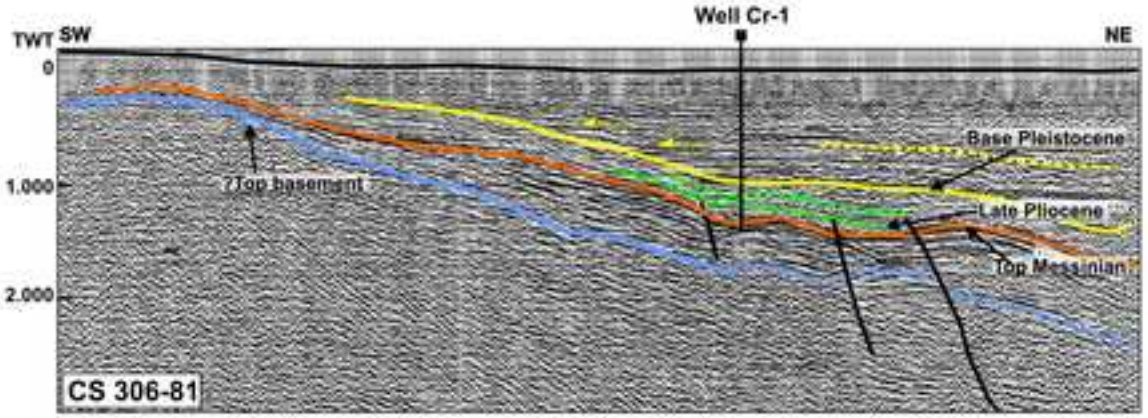
Well Cr-1
TWT
SW
NE
0
1.000
2.000
?Top basement
Base Pleistocene
Late Pliocene
?Top Messinian
CS 306-81

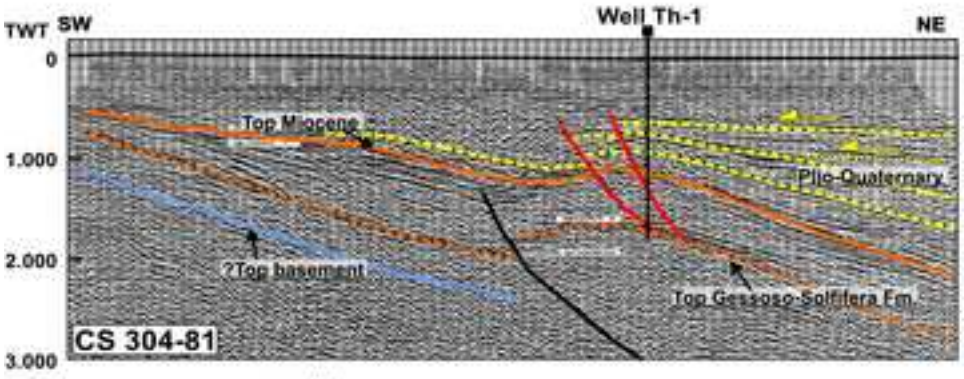
Well Th-1
TWT
SW
NE
0
1.000
2.000
3.000
Top Miocene
Plio-Quaternary
?Top basement
Top Gessoso-Solfifera Fm.
CS 304-81

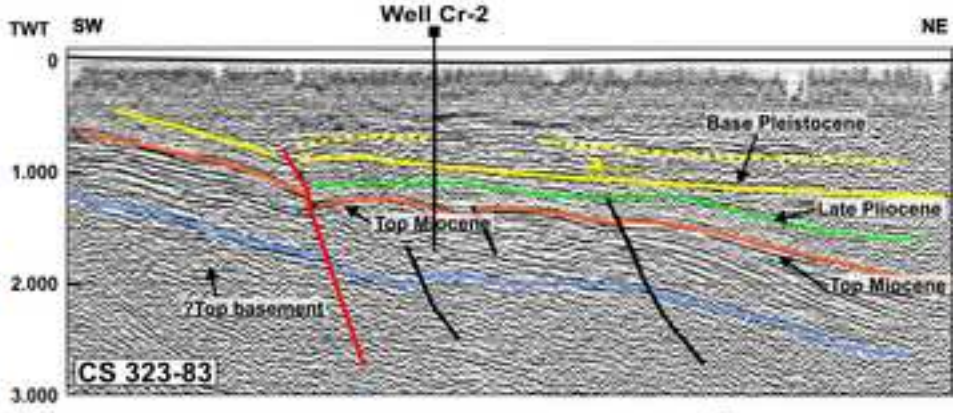
Well Cr-2
TWT
SW
NE
0
1.000
2.000
3.000
Base Pleistocene
Late Pliocene
Top Miocene
?Top basement
Top Miocene
CS 323-83

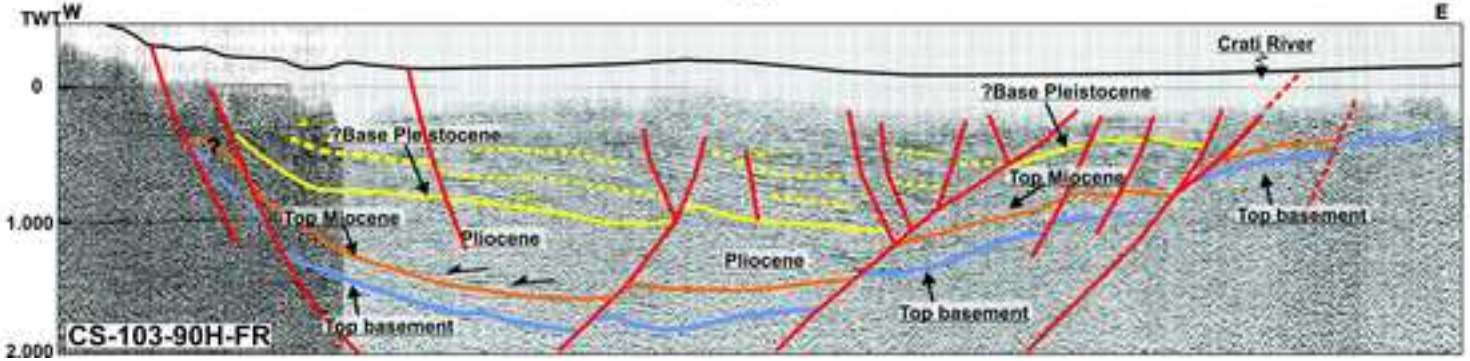
TWT
W
E
0
1.000
2.000
Crati River
?Base Pleistocene
?Base Pleistocene
Top Miocene
Top Miocene
Pliocene
Pliocene
Top basement
Top basement
Top basement
CS-103-90H-FR

Figure

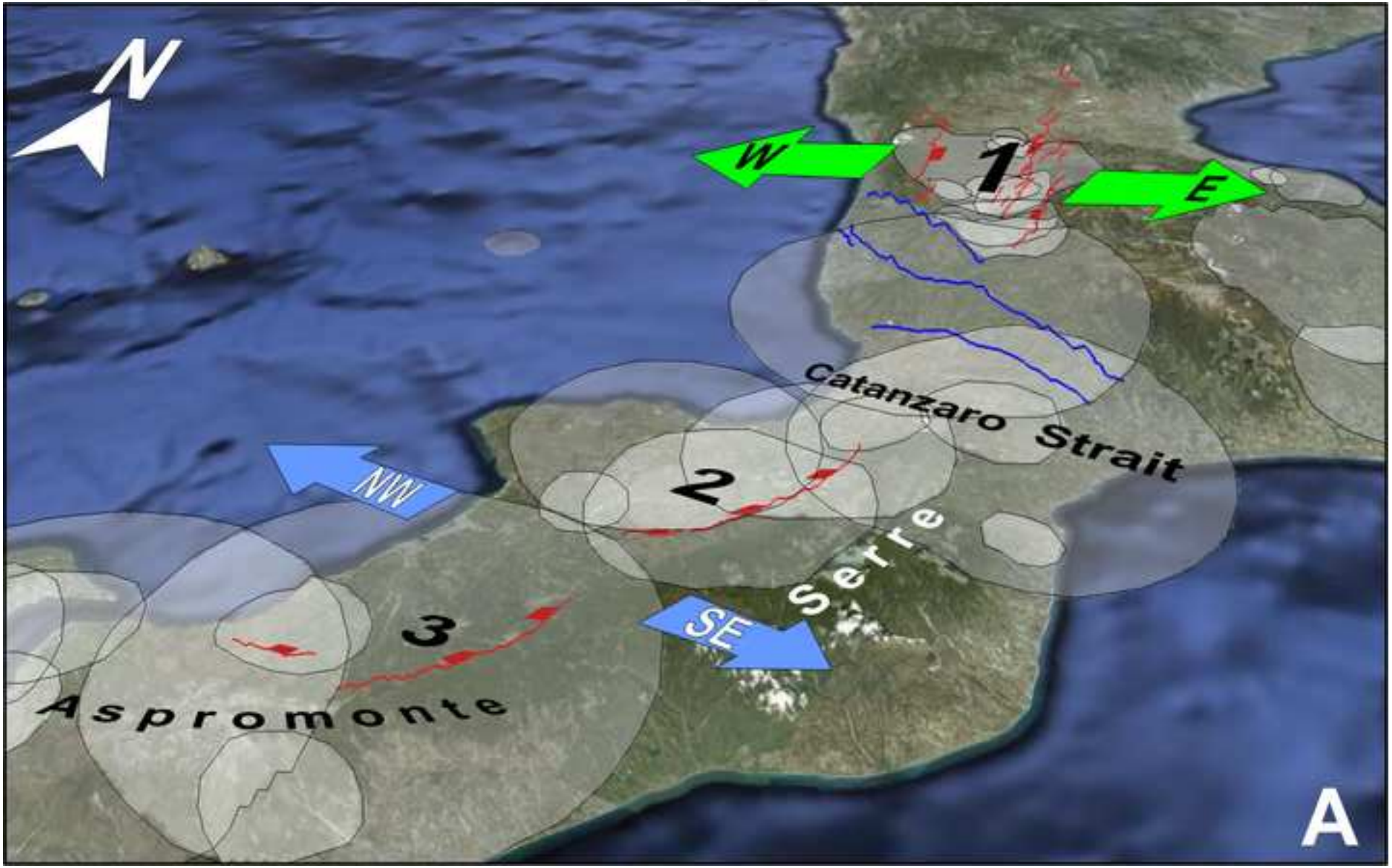

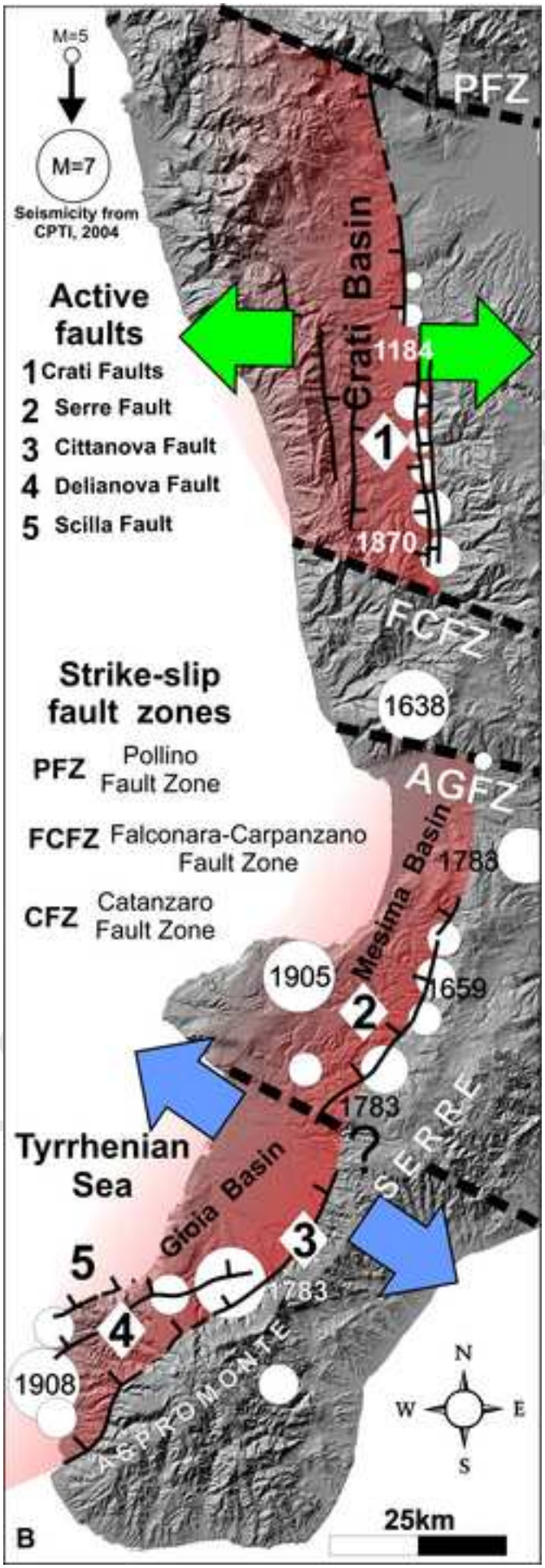

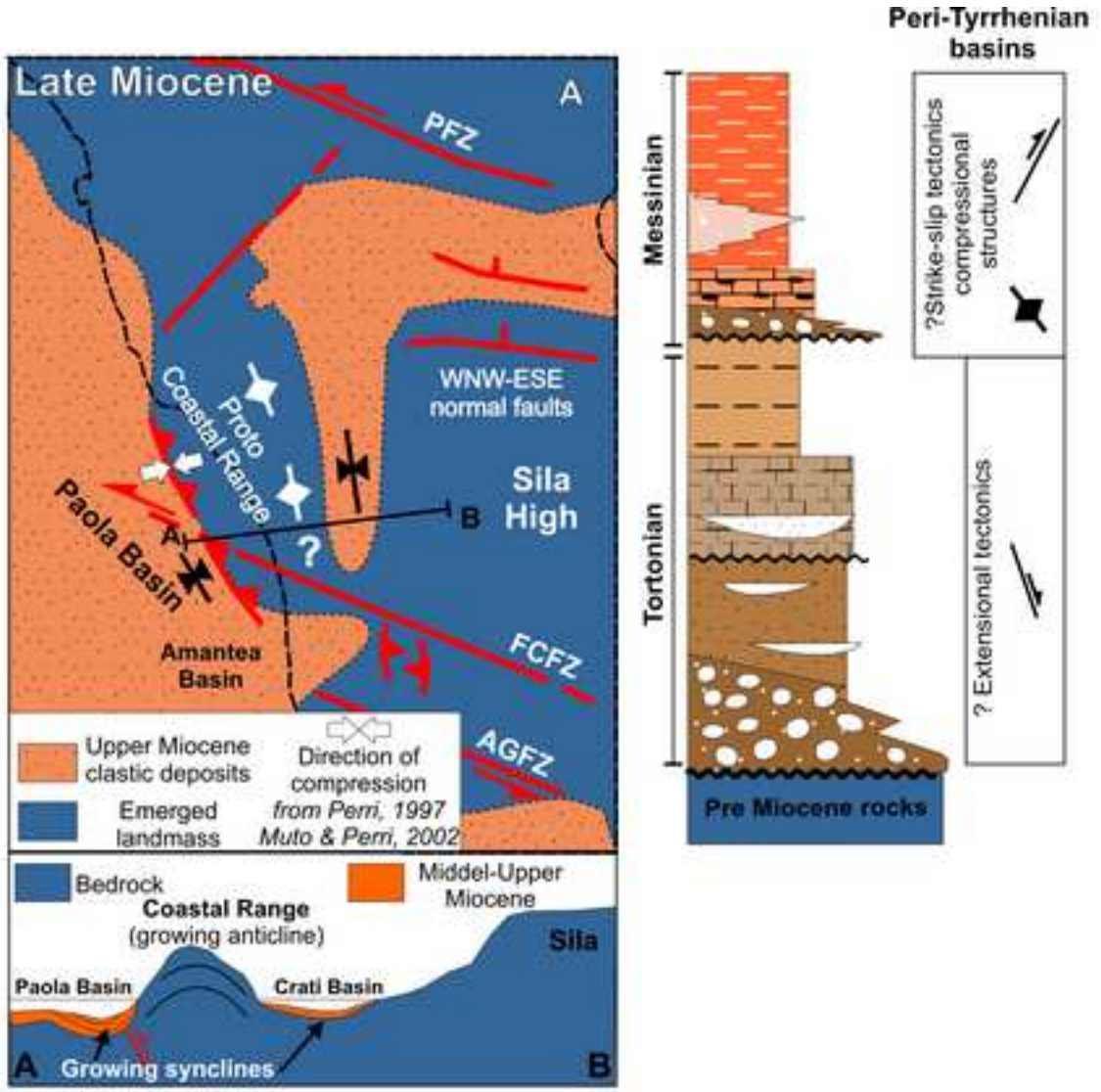

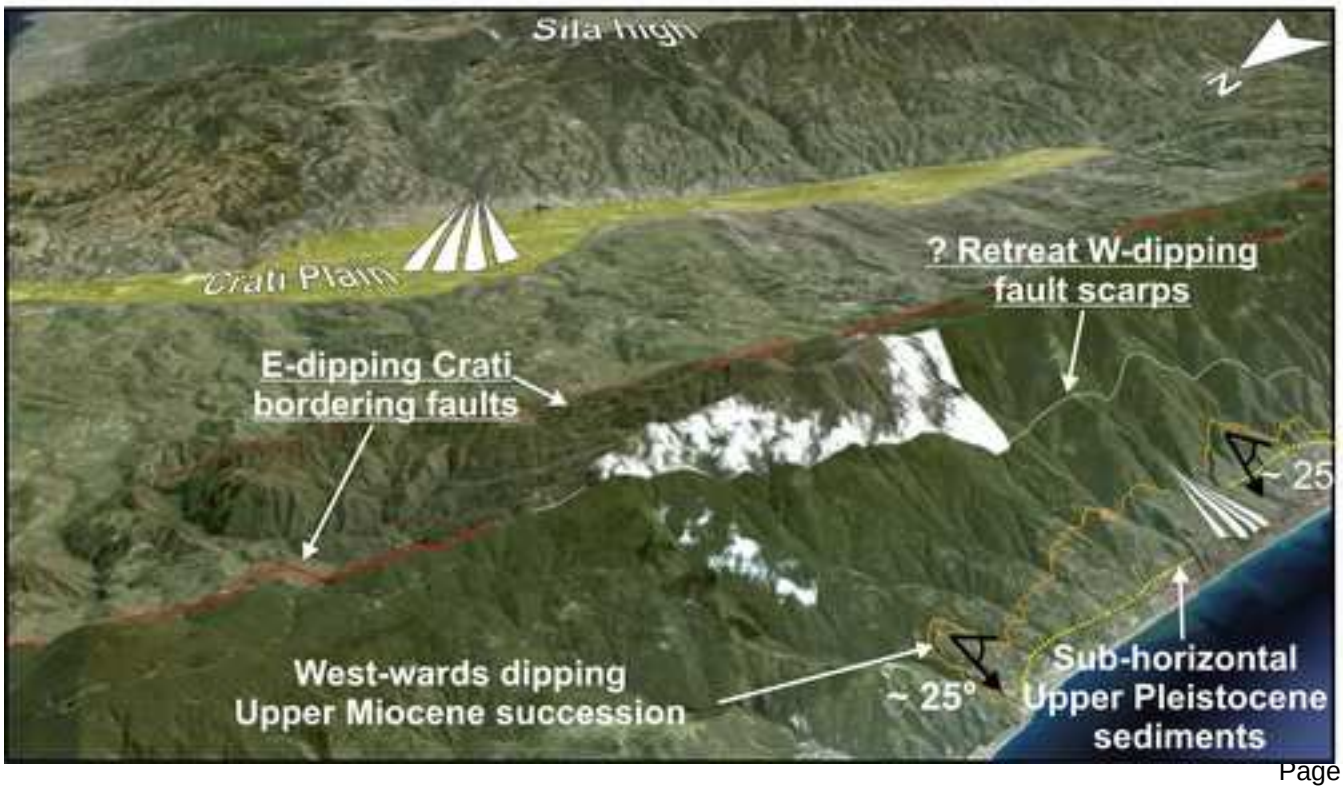

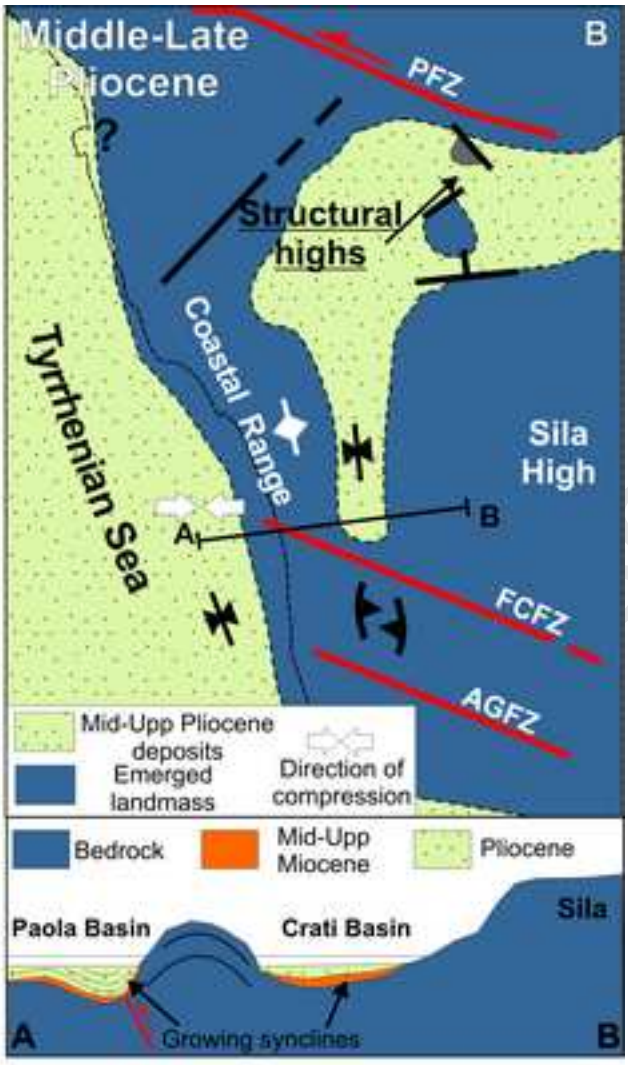

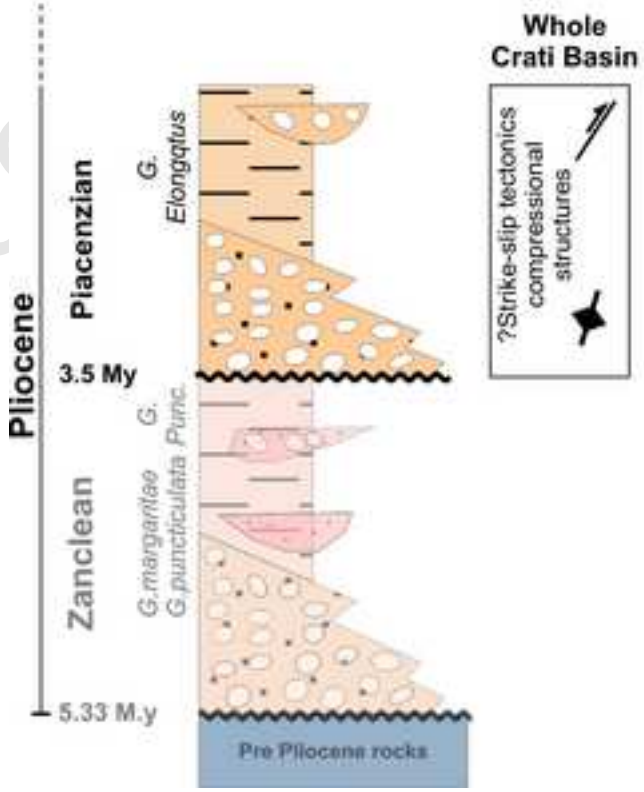

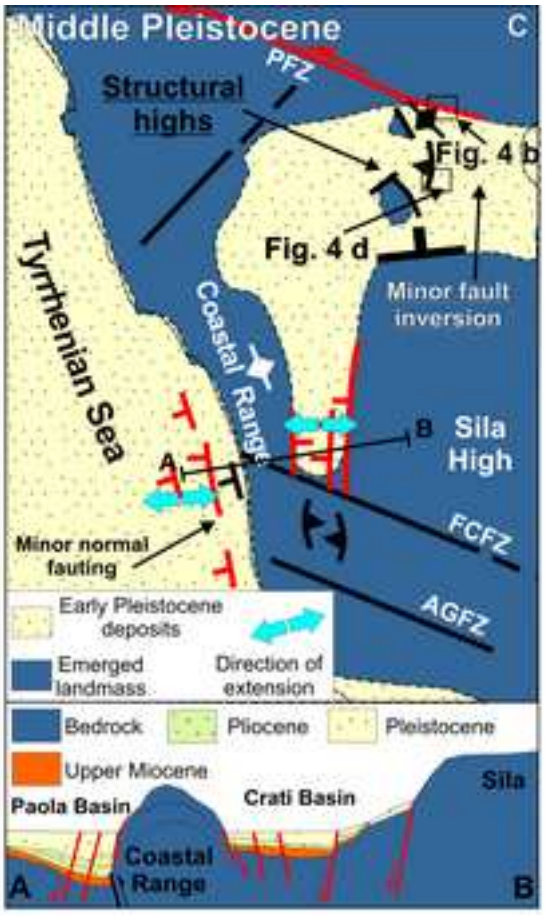

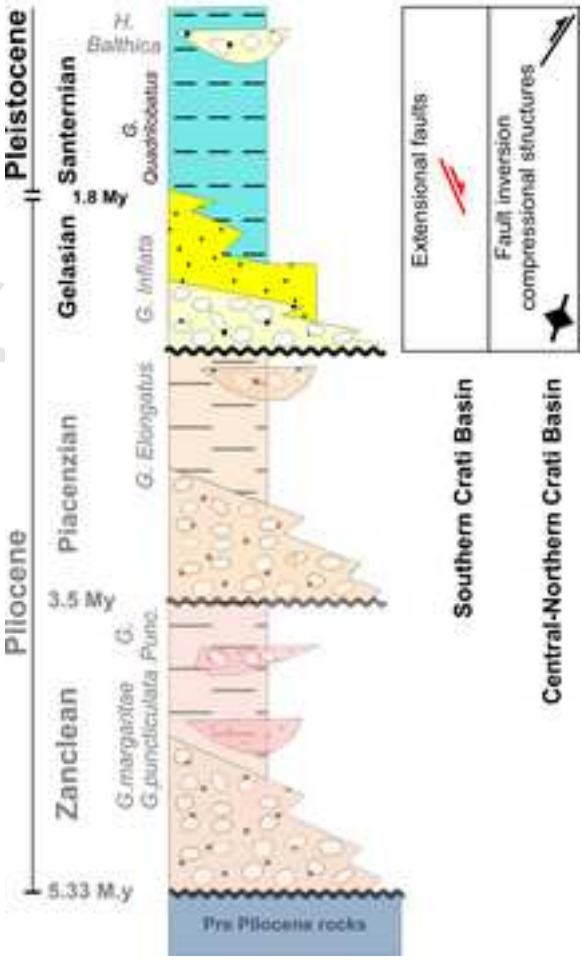

Figure

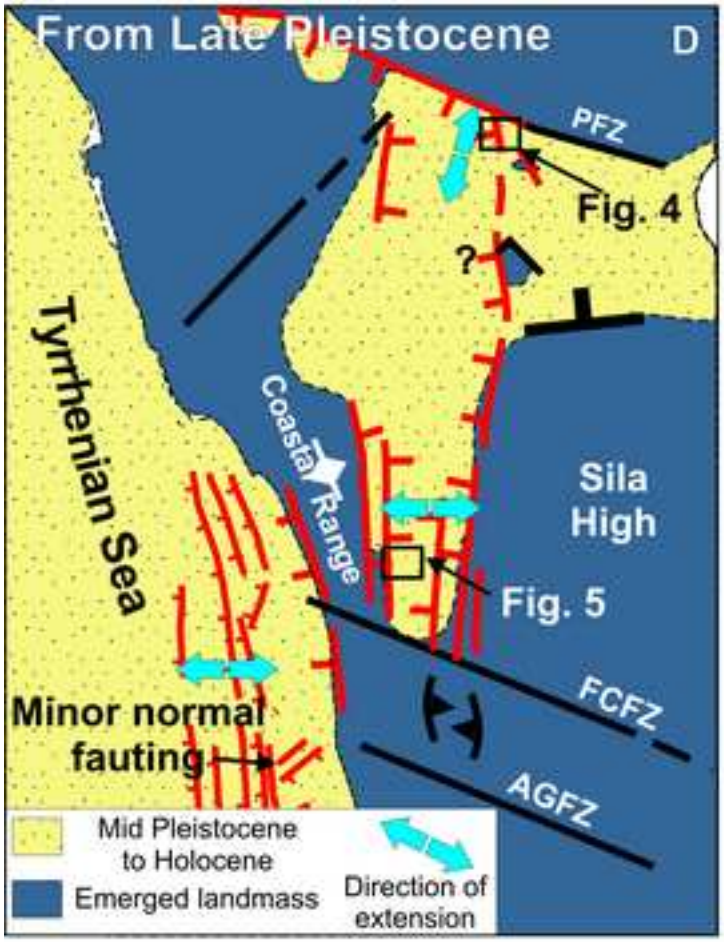
From Late Pleistocene
D
PFZ
Fig. 4
?
Tyrrhenian Sea
Coasta Range
Sila High
Fig. 5
FCFZ
Minor normal fauting
AGFZ
Mid Pleistocene to Holocene
Emerged landmass
Direction of extension

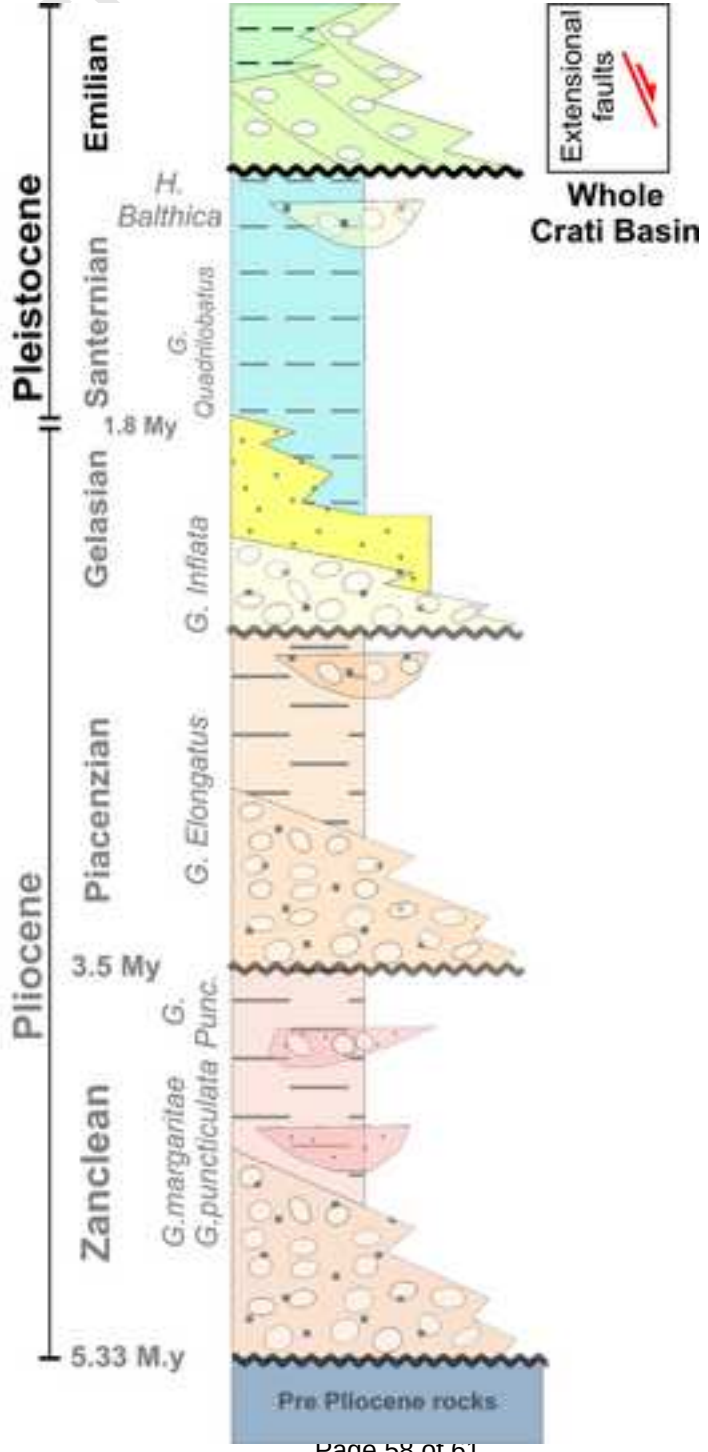
Pleistocene
Pliocene
Emilian
Santernian
Gelasian
Piacenzian
Zanclean
1.8 My
3.5 My
5.33 M.y
H. Balthica
G. Quadrilobatus
G. Inflata
G. Elongatus
G. G.margaritae G.puncticulata Punc.
Extensional faults
Whole Crati Basin
Pre Pliocene rocks

Figure

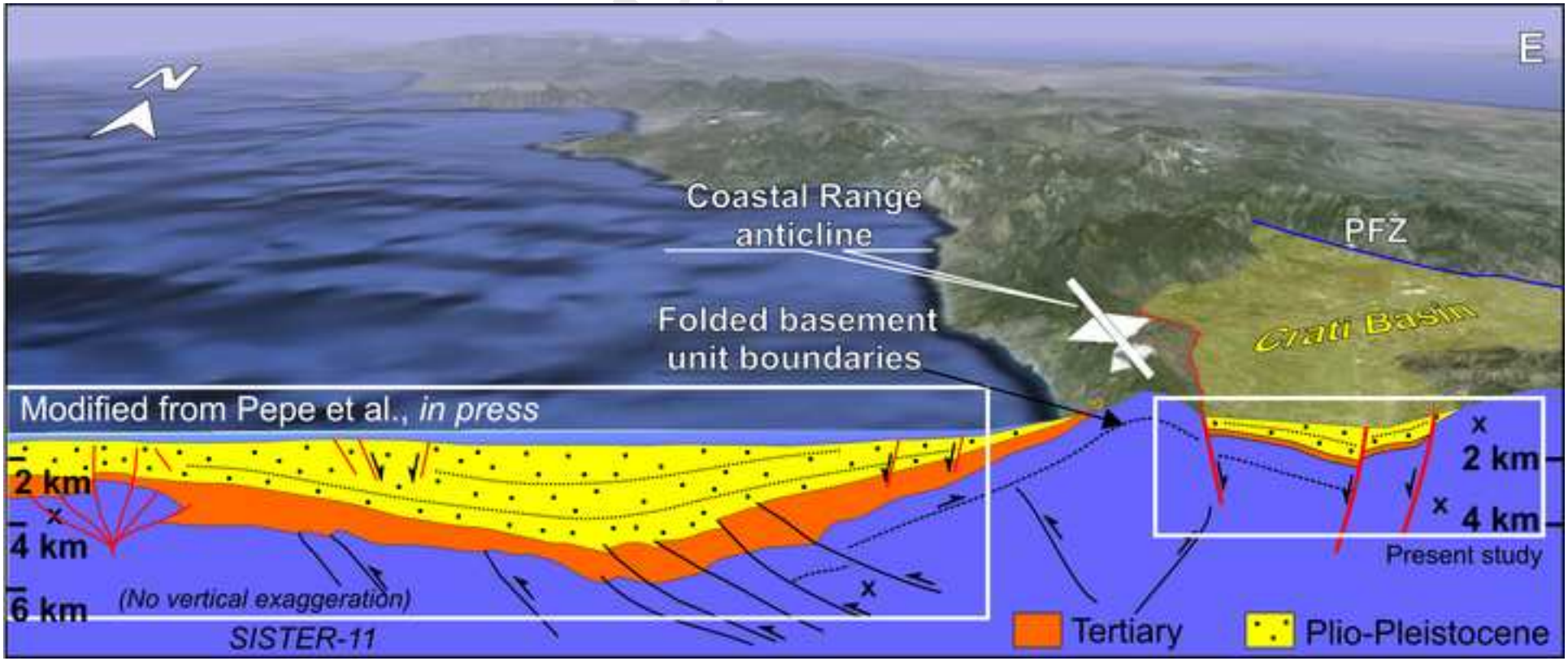
E
Coastal Range
anticline
PFZ
Folded basement
unit boundaries
Cauca Basin
Modified from Pepe et al., in press
2 km
4 km
6 km
(No vertical exaggeration)
SISTER-11
2 km
4 km
Present study
Tertiary
Plio-Pleistocene

Figure

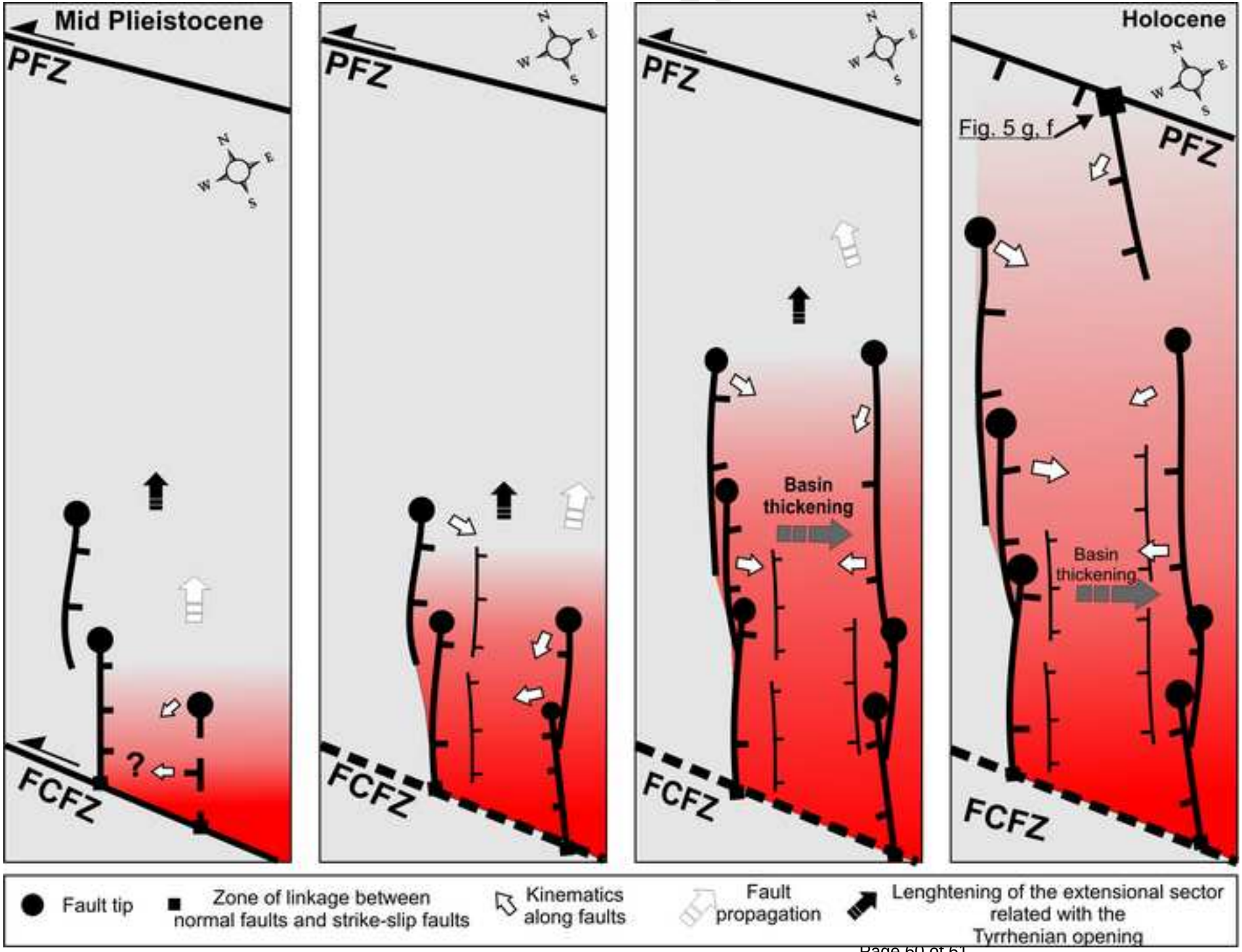
Mid Plieistocene
PFZ
FCFZ
?
Basin thickening
Holocene
Fig. 5 g, f
Basin thickening
Fault tip
Zone of linkage between normal faults and strike-slip faults
Kinematics along faults
Fault propagation
Lenghtening of the extensional sector related with the Tyrrhenian opening

Section 1
Globigerina bulloides
Globigerinoides extremus
Globigerinoides obliquus
Globigerinoides quadrilobatus
Globorotalia margaritae
Globorotalia punticulata
Globorotalia siakensis
Orbulina universa
Age: **ZANCLEAN**; biozone: *Margaritae puncticulata* (MPL3)

Section 2
Globigerina apertura
Globigerina bulloides
Globigerina decoraperta
Globigerina falconensis
Globigerina quinqueloba
Globigerina sp.
Globigerinoides conglobatus
Globigerinoides elongatus
Globorotalia crassaformis
Orbulina universa
Age: **PIACENZIAN**; biozone: *Globigerinoides elongatus* (MPL5a)

Section 3
Globigerina bulloides
Globigerina borealis
Globigerina falconensis
Globigerina quinqueloba
Globigerina sp
Globigerinita glutinata
Orbulina universa
Age: **?GELASIAN**; biozone: *Globorotalia inflata* (MPL 6)